TAMPEREEN TEKNILLINEN YLIOPISTO
TAMPERE UNIVERSITY OF TECHNOLOGY

PRAKASH SUBEDI

# SOFTWARE SIMULATOR AND SIGNAL ANALYSIS FOR GALILEO E5 BAND SIGNALS

Master of Science Thesis

Examiners: Assoc. Prof. Dr. Elena-Simona Lohan
Dr. Jie Zhang
Dr. M. Zahidul H. Bhuiyan
Supervisors: Assoc. Prof. Dr. Elena-Simona Lohan
Dr. Jie Zhang
Examiners and topic approved by the Faculty Council of the Faculty of Computing and Electrical Engineering on 9th October 2013.

# ABSTRACT

TAMPERE UNIVERSITY OF TECHNOLOGY
Master's Degree Programme in Electrical Engineering
**SUBEDI, PRAKASH:** Software Simulator and Signal Analysis for Galileo E5 band Signals
Master of Science Thesis, 63 pages
October, 2013
Major: Radio Frequency Electronics
Examiners: Assoc. Professor Dr. Elena-Simona Lohan
Dr. Jie Zhang
Dr. Mohammad Zahidul Hasan Bhuiyan
Keywords: Galileo, GNSS Receiver, Acquisition, Tracking

Galileo is the European Global Navigation Satellite System (GNSS) that aims at providing high availability, increased accuracy, and various location services under the civilian control. Four in-orbit validation satellites have already been launched till date and the system is estimated to be fully deployed by the year 2020. The Galileo navigation signals are transmitted at four frequency bands, which are named E5a, E5b, E6, and E1 bands. The signal of interest in this thesis is Galileo E5a band and Galileo E5b band signals.

Signal acquisition and signal tracking are the main functions in a GNSS receiver. Acquisition identifies all the visible satellites and estimates the coarse values of carrier frequency and code phase estimates of the satellite signal. Tracking refines the coarse carrier frequency and code phase estimates, and keeps track of the satellite. The objective of this thesis has been to design and implement Galileo E5a and E5b signals receiver which can acquire all the visible E5a and E5b signals and which gives coarse estimate of carrier frequency and code phase. Such a receiver has been successfully designed in Matlab starting from the Matlab initial files provided by the Finnish Geodetic Institute (FGI) provided tool.

In this thesis, two different software implementations are analyzed: 1) The acquisition and tracking of simulated Galileo E5a signals generated in the Matlab Simulink E1-E5 model; and 2) The acquisition of real-time Galileo E5b signals received from the satellite provided by Finnish Geodetic Institute (FGI), Masala, Finland. In the Simulink implementation, the whole E5 signal is generated and propagated through different channel profiles. The received signals are tested with acquisition and tracking and the results are compared for different channel profile and Carrier-to-Noise density ratio. Similarly, the real-time Galileo signals from four satellites now available on sky from the Galileo constellation were received and performed acquisition. In both implementations, a sharp triangular peak was observed at the rough frequency and code phase estimates, proving that the Galileo E5a/b signals can be indeed acquired correctly with the implemented simulator.

# PREFACE

This Master of Science Thesis has been written for Department of electrical Engineering at the Tampere University of Technology (TUT), Tampere, Finland. This thesis work has been carried out in the Signal Processing for wireless positioning group at the Department of Electronics and Communications Engineering during the year 2013-2014.

The work presented in this thesis would not have this form without the support of many people. First of all, I would like to thank Assoc. Prof. Dr. Elena-Simona Lohan, and Finnish Geodetic Institute (FGI), Masala, Finland for providing me the thesis topic. I would like to express my deepest gratitude to my supervisors and examiners, Assoc. Prof, Dr. Elena-Simona Lohan and Dr. Jie Zhang, for providing me the dedication, continuous support, guidance, encouragement, and valuable feedbacks throughout the entire duration of the thesis. I would like to extend my gratitude to my examiner Dr. Mohammad Zahidul Hasan Bhuiyan from Finnish Geodetic Institute for his support throughout the research work. I would also like to express my appreciation to my Nepalese friends in Tampere for continuous encouragement and moral support whenever I needed. Special thanks to my friends Udhyan Timilsina, Anil Baniya, Dipesh Paudel, Nirajan Pant, and Sandeep Shrestha for their great concerning and encouragement.

Last but not least, I am in debt to my family for their unconditional love and endless inspiration. I would not have been able to complete my Master's Degree without their support. I want to dedicate this thesis to my family.

Tampere, Finland

Prakash Subedi

# Contents

## LIST OF ABBREVIATIONS

| | |
|---|---|
| ADC | Analog-to-Digital Converter |
| AGC | Automatic Gain Control |
| A-GPS | Assisted Global Positioning System |
| A-GNSS | Assisted Global Navigation Satellite System |
| AltBOC | Alternative Binary Offset Carrier |
| ARNS | Aeronautical Radio Navigation Services |
| ASIC | Application Specific Integrated Circuits |
| BDS | BeiDou System |
| BOC | Binary Offset Carrier |
| bps | bits per second |
| BPSK | Binary Phase Shift Keying |
| C/A | Coarse/Acquisition |
| CBOC | Composite Binary Offset Carrier |
| CosBOC | Cosine Binary Offset Carrier |
| CDMA | Code Division Multiple Access |
| CRC | Cyclic Redundancy Check |
| CS | Commercial Service in Galileo |
| CS | Control Segment in GPS |
| dBW | decibel Watts |
| DoD | Department of Defense |
| DGPS | Differential Global Positioning System |
| DLL | Delay Lock Loop |
| DSP | Digital Signal Processor |
| E | Early correlator |
| EC | European Commission |
| EML | Early-Minus-Late |
| ESA | European Space Agency |
| EU | European Union |
| Etc | et cetera |
| FAA | Federal Aviation Agency |
| FDMA | Frequency Division Multiple Access |
| FEC | Forward Error Correction |
| FGI | Finnish Geodetic Institute |
| FLL | Frequency Lock Loop |
| FPGA | Field-Programmable Gate Array |
| GCC | Galileo Control Center |
| GEO | Geostationary Orbit |
| GLONASS | GLObal NAvigation Satellite System |
| GNSS | Global Navigation Satellite System |
| GPS | Global Positioning System |

| | |
|---|---|
| GSS | Galileo Sensor Stations |
| ICAO | International Civil Aviation Organization |
| IF | Intermediate Frequency |
| IGSO | Inclined Geosynchronous Satellite Orbit |
| IOV | In-orbit Validation |
| JMA | Japanese Meteorological Agency |
| L | Late correlator |
| LBS | Location-based Service |
| LFSR | Linear Feedback Shift Register |
| LO | Local Oscillator |
| MBOC | Multiplexed Binary Offset Carrier |
| MCS | Master Control Station |
| MEO | Medium Earth Orbit |
| MMI | Multi Media Interface |
| ms | millisecond |
| MTSAT | Multifunctional Transport Satellites |
| NCO | Numerically Controlled Oscillator |
| NLOS | None Line Of Sight |
| ns | nanosecond |
| NSR | Navigation Software Receiver |
| OS | Open Service |
| PLL | Phase Lock Loop |
| PRN | Pseudo-Random Noise |
| PRS | Public Regulated Service |
| PSD | Power Spectral Density |
| PVT | Position, Velocity, Time |
| RF | Radio Frequency |
| RFI | Radio Frequency Interference |
| RNSS | Radio Navigation Satellite Services |
| SBAS | Satellite Based Augmentation System |
| SinBOC | Sine Binary Offset Carrier |
| SoL | Safety-of-Life Service |
| sps | symbols per second |
| sv | satellite vehicle |
| STF | Signal Task Force |
| TEC | Total Electron Content |
| TOA | Time Of Arrival |
| TMBOC | Time-Multiplexed Binary Offset Carrier |
| TTFF | Time To First Fix |
| TUT | Tampere University of Technology |
| USSR | Union of Soviet Socialist Republics |

# LIST OF SYMBOLS

| | |
|---|---|
| $C_{E1}$ | Unencrypted Galileo E1 ranging code |
| $C_{E5}$ | Unencrypted Galileo E5 ranging code |
| $C_{k,n}$ | $k^{th}$ chip corresponding to the $n^{th}$ symbol |
| $D_{E1}$ | Galileo E1 Navigation data stream |
| $D_{E5}$ | Galileo E5 Navigation data stream |
| $G_{AltBOC}(f)$ | Unit-power PSD of AltBOC modulation |
| $G_{BPSK}(f)$ | PSD of BPSK modulation |
| $G_{CosBOC}(f)$ | Unit-power PSD of CosBOC modulation |
| $G_{MBOC}$ | PSD of MBOC modulation |
| $G_{SinBOC}(f)$ | Unit-power PSD of SinBOC modulation |
| $I_E$ | In-phase component of Early correlator |
| $I_L$ | In-phase component of Late correlator |
| $I_P$ | In-phase component of Prompt correlator |
| $N_{BOC}$ | BOC modulation order |
| $Q_E$ | Quadrature-phase component for Early correlator |
| $Q_L$ | Quadrature-phase component for Late correlator |
| $Q_P$ | Quadrature-phase component for Prompt correlator |
| $S_F$ | Spreading factor |
| $S_{SinBOC}(t)$ | SinBOC signal waveform |
| $S_{cosBOC}(t)$ | CosBOC signal waveform |
| $S_{sinBOC}(t)$ | SinBOC signal waveform |
| $T_{B_1}$ | Sub-chip interval after the first modulation stage |
| $T_B$ | Sub-chip interval after the second modulation stage |
| $T_c$ | Chip period |
| $T_{sym}$ | Symbol period |
| $b_n$ | $n^{th}$ complex data symbol |
| $f_c$ | Chip rate of primary code of Galileo signal |
| $f_{cs}$ | Chip rate of secondary code of Galileo signal |
| $f_{sc}$ | Sub-carrier frequency |
| $x_j$ | $j^{th}$ satellite latitude |
| $x_u$ | User latitude |
| $y_j$ | $j^{th}$ satellite longitude |
| $y_u$ | User longitude |
| $z_j$ | $j^{th}$ satellite altitude |
| $z_u$ | User altitude |
| $\delta_t$ | Clock bias |
| $\rho_i$ | Pseudorange measurement |

| | |
|---|---|
| $\otimes$ | Convolution operator |
| $\Delta f$ | Frequency search resolution |
| $c$ | Speed of light |
| $d(t)$ | Data sequence after spreading |
| $K$ | Frequency channel of the signals transmitted by GLONASS satellites |
| $sign(\cdot)$ | Signum operator |
| $w$ | Amplitude weighting factor |
| $C/N_0$ | Channel to Noise Density Ratio |
| $\delta(t)$ | Discrete Dirac pulse |

## LIST OF FIGURES

# LIST OF TABLES

# 1. INTRODUCTION

## 1.1. GNSS in general

Navigation, in general, is defined as the science of getting a craft or person from one place to another. A satellite navigation system is a system of satellites that provide independent geo-spatial positioning with global coverage. Satellite-based positioning is focusing on the determination of positions of the receivers of interest on land or at sea, in the air and in space by means of artificial satellites. The International Civil Aviation Organization (ICAO) defines Global Navigation Satellite System (GNSS) as "a worldwide position and time determination system that includes one or more satellite constellations, aircraft receivers and system integrity monitoring, augmented as necessary to support the required navigation performance for the intended operation". It consists of the set of all satellite constellations orbiting at about twenty thousand kilometers altitude over the earth surface, continuously transmitting signals to users enabling them to determine their three-dimensional position with global coverage [1]. In general, satellites broadcast two types of data, almanac and ephemeris. Almanac is a set of data that every satellite transmits. It includes information about the satellite health and course orbital parameters for all satellite vehicles (sv). Ephemeris data contains precise orbital and clock correction for each sv. It is necessary for precise positioning. GNSS can be classified according to global coverage systems in the U.S. Global Positioning System (GPS), Russian GLONASS, European Galileo, Japanese Quasi Zenith Satellite System and Chinese Compass.

### 1.1.1. Global Positioning System (GPS)

GPS is a GNSS owned by United States and developed by the U.S. Department of Defense (DoD) in 1973[2]. Initially, GPS was targeted for the military purposes to accurately determine the position, velocity and time. Later on, it was made available for civilian use [5]. Some civilian fields that use GPS include aircraft navigation systems, automotive applications, cellular phone, marines and hand-held receivers used by campers and hikers.

GPS is composed of three segments: space, control and user equipment segments. Space segment consists of 32 constellation satellites distributed in six orbital planes. Space segment provides the radio signal to the user equipment. Control segment (CS) controls the proper functioning of satellites and their orbital configuration. It monitors the navigation signal from space segment to user and updates the navigation message. Furthermore, the control segment monitors each satellite's health, battery charging and

updates the satellite clock corrections everyday.[2] CS consists of three physical components: master control station (MCS), monitor stations and the ground antennas. The task of CS is divided into these three physical components. The user segment is a GPS receiver which receives the downlink signal from the space segment.

Each GPS signal is composed of *carrier, navigation data* and *spreading sequence*. The *Carrier* carries the carrier frequency. The *Navigation data* contain the satellite information. The *spreading sequence* is a pseudo-random sequence of bits that is modulated with carrier frequency. It does not hold any satellite information. Each satellite has two unique spreading codes, namely the coarse acquisition code (C/A) and the precision code (P(Y)). The C/A code is a sequence of 1023 chips which is freely available to the public [3]. C/A code has a chip rate of 1.023 MHz.

Each GPS satellite transmits three GPS signals, with radio frequencies in UHF band (500 MHz to 3 GHz). Referring to [3], the operating frequencies are

$$f_{L1} = 1575.42\ MHz$$
$$f_{L2} = 1227.60\ MHz$$
$$f_{L5} = 1176.45\ MHz$$

where L1, L2 and L5 denotes the carrier waves of GPS signal. All the satellite transmits the navigation message at these frequencies and uses CDMA spread spectrum technique. The L1 carrier is modulated by both the C/A and P(Y) codes, while the L2 carrier is only modulated by the P(Y) code [2]. The signal component L5 is the international Safety of Life signal for aviation, developed in the GPS modernization program, to strengthen GPS availability, integrity, accuracy and robustness to interference.

Besides L5, the government is in the process of fielding two new signals, namely L1C and L2C. The L2C signal enables dual frequency to increase position accuracy and provide fast location. The L1C signal is the interoperability signal that establishes a common signal between the GPS and other space based positioning, navigation, and timing systems for the benefit of the civil users around the world. Moreover, L1C signal provides compatibility between the GPS and other GNSS systems available.

### 1.1.2. GLONASS

GLONASS (GLObal NAvigation Satellite System) is the GNSS, initially operated by the former Union of Soviet Socialist Republics (USSR) in the mid-1970s [5]. Similar to GPS, it provides three dimensional position, velocity measuring and timing anywhere in the world. Russian military force operated GLONASS initially for military purpose. In 1988, a meeting with Special Committee on Future Air Navigation Systems of the International Civil Aviation Organization (ICAO) was held and GLONASS was provided for free for the civilian use [5].

On October 12, 1982, the USSR launched first satellite [2]. During the test scenario, in the first phase (1983-1985), four satellites were successfully deployed. In the second phase (1986-1993), 8 satellites were added in the constellation. Thus, the tests were completed and on September 24, 1993, The President of the Russian Federation de-

clared GLONASS to be operational [2]. After about three years, on January 18, 1996, GLONASS was fully operated with 24 satellites in the constellation. However, the GLONASS system fell into disrepair with the collapse of the Russian economy and the reduction in funding for space industry. In the early 2000s, under Vladimir Putin's presidency, the government prioritised to restore the system and the funding was substantially increased. In May 2007, Russian President Vladimir Putin signed a decree on the GLONASS navigation system to provide the service free of charge for customers.

Similar to GPS, GLONASS is composed of space, control and user equipment segments. The completely deployed GLONASS constellation will consist of 31 satellites separated in three orbital planes. Each satellite is situated at a distance of 19,100 Km from the earth's surface and each satellite completes the orbit in approximately 11 hours and 15 minutes [2; 6]. Currently, 24 satellites are operational, 3 satellites are "active on-orbit spares" and one satellite each is "in maintenance" and "in flight tests phase" [50]. CS of GLONASS has a similar function as that of GPS. It is used to track and to monitor the status of satellites, and to upload the ephemeris, clock correction and almanac information into each GLONASS satellite. The task includes synchronizing the satellite clock with GLONASS system time and calculating the offset between GLONASS system time and UTC. User equipment segment receives and process the signal broadcasted by the satellites and determines the user position, velocity and precise time.

GLONASS uses Frequency Division Multiple Access (FDMA) to transmit the satellite signals unlike the GPS which uses CDMA. Traditionally, GLONASS satellite transmits two signals in radio frequency sub-band L1~1602 MHz and L2~1246 MHz. Referring to [6], the nominal values of L1 and L2 carrier frequencies are defined by the following expressions:

$$f_{K1} = f_{01} + K\Delta f_1$$
$$f_{K2} = f_{02} + K\Delta f_2$$

where, K is a frequency number (frequency channel) of the signals transmitted by GLONASS satellites in the L1 and L2 sub-bands, and

$$f_{01} = 1602\,MHz;\ \Delta f_1 = 562{,}2\,KHz, for\ sub-band\ L1;$$
$$f_{02} = 1246\,MHz;\ \Delta f_1 = 437{,}5\,KHz, for\ sub-band\ L2;$$

Channel number K for any particular GLONASS satellite and the nominal values of carrier frequencies $f_{K1}$ and $f_{K2}$ for channel numbers K are provided in GLONASS-ICD document [6].

Unlike the GPS, each GLONASS satellite transmits same the PRN code pair on a different frequency which is modulated to the carrier frequency using BPSK [2].

### 1.1.3. BeiDou -2/Compass

BeiDou Navigation Satellite System (BDS) is a Chinese Satellite System established in 1994 under sponsorship of the General Staff of the Central Committee of the People's Liberation Army (CCPLA) Mapping Bureau. BDS is designed to provide positioning, time and fleet-management to Chinese military and civilians. The first two test satellites were launched in October and December 2000. The third satellite was launched in May 2003. Referring [7], after the completion, the BeiDou space constellation consists of five Geostationary Earth Orbit (GEO) satellites, twenty-seven Medium Earth Orbit (MEO) satellites and three Inclined Geosynchronous Satellite Orbit (IGSO) satellites. Beidou is planned to provide two services. Open service with accuracies of 10 m in positioning, 0.2 m/s in velocity, and 50 nS in time dissemination [1]. The second service is intended for the Chinese government. By the end of 2013, the constellation consists of fourteen operational BeiDou satellites [7]. The BeiDou satellite transmits the satellite signal in two carrier frequencies B1I and B2I. The nominal frequency of B1I is 1561.098 MHz, and the nominal frequency of B2I signal is 1207.140 MHz. the transmitted signal is modulated by Quadrature Phase Shift Keying (QPSK) modulation [7].

### 1.1.4. Galileo

Galileo is European's own global Navigation System that will provide highly accurate and guaranteed global positioning service under the civilian control. The frequency structure and signal design of Galileo is developed by the European Commission's Galileo Signal Task Force (STF) which was established by the European Commission (EU) member states in March 2001 [9]. Galileo is designed to be inter-operable with GPS and GLONASS. European Space Agency has launched the first four In-Orbit Validation (IOV) satellites on 21 October 2011 and 12 October 2012 [47]. The Galileo system is expected to be fully operational in 2019/2020.

The Galileo system also consists of space, control and user equipment segment. The main function of the Galileo Space Segment includes the generation and transmission of code and carrier phase signals with a specific Galileo signal structure, and the storage and retransmission of the navigation message sent by the Control Segment. When fully deployed, the space segment will consist of 30 satellites with 27 operational and 3 spare satellites, positioned in Medium Earth Orbit (MEO) in three circular planes. The Galileo satellites are situated at an altitude of 23,222 Km from the earth's surface and at an inclination of the orbital planes of 56 degrees with reference to the equilateral plane. The Galileo Control Segment (GCS) controls and maintains the status and configuration of satellite constellation, predict ephemeris and satellite clock evolution, updates the navigation messages for all the satellites and synchronizes the satellite time with GNSS time scale. The GCS is composed of two Ground Control Centres (GCC), a network of Telemetry, Tracking and Control (TT&C) stations, a network of Mission Uplink Stations (ULS), and a network of Galileo Sensor Stations (GSS) [51]. The Galileo User Segment

consists of Galileo receivers. The main task of the User Segment is to receive Galileo signals, determine pseudoranges, and solve the navigation equations in order to obtain their coordinates and provide a very accurate time.

The detailed description about Galileo frequency plan is explained in chapter 4. Table 1.1 summarizes the different GNSS systems.

***Table 1.1.*** *Global Navigation System Status*

| | **GPS** | **GALILEO** | **GLONASS** | **BeiDou** |
|---|---|---|---|---|
| **First Launch** | 1978 (by US Department of Defense) | 2011 (European Union, EU) | 1982 (Union of Soviet Socialist Republics, USSR) | 2007 (China) |
| **Full Operational Capability (FOC)** | 1995 | 2018 | 2011 | 2020 |
| **Number of satellites** | 32 | 30 | 31 | 35 |
| **Orbital planes** | 6 | 3 | 3 | 3 |
| **Access Scheme** | CDMA | CDMA | FDMA/CDMA | CDMA |
| **Current Status** | 31 operational, 1 in commissioning phase | 4 IOV satellites, 22 operational satellites budgeted | 24 operational, 1 in preparation, 2 on maintenance, 3 reserved and 1 on test | 14 operational satellites, full coverage on Asia pacific region |

## 1.2. Assisted GNSS

A network-assisted GNSS (A-GNSS) method is developed to simultaneously reduce the time of a positioning solution and to increase the sensitivity of the GNSS receiver in cellular network [2]. GNSS satellites are limited in the amount of power they can provide to users on the ground. Thus, A-GNSS helps to improve the processing power of the GNSS receiver by means of separate communication channel, so that they can operate successfully in disadvantaged locations and circumstances where buildings, trees, hills may partially degrade the GNSS signals [28]. It can be any of the systems GPS, GLONASS, Galileo and COMPASS or combination between them.

A standard GNSS receiver takes long time to demodulate the satellite orbit parameters and satellite clock correction parameters directly from the satellites. Even if a GNSS receiver could acquire the satellites instantly, it would still need some additional 18-30 seconds of continuous tracking to demodulate navigation data message to extract the required orbital elements and satellite clock correction terms for each satellite. As the GNSS receiver is developed for the purpose of emergency response system, so it is not feasible to wait for the applications (such as in mobile phones and personal naviga-

tion devices) for 30 seconds to demodulate the data. Thus, A-GNSS is developed to improve the standard GNSS performance by providing additional information from cellular networks, through an alternative communication channel communication instead of sending directly from the satellites themselves. The A-GNSS decreases the acquisition time of the weak signals as well as it may eliminate the need for the data demodulating process [2; 27; 28].

Figure 2.2 shows overview of an A-GNSS system. In this figure, the satellite data is collected and processed by an A-GNSS network and location server. The assistance data is usually provided through a wireless network, most commonly over a cellular data channel. The approximate position of the A-GNSS receiver is usually derived from a database of cellular tower locations.

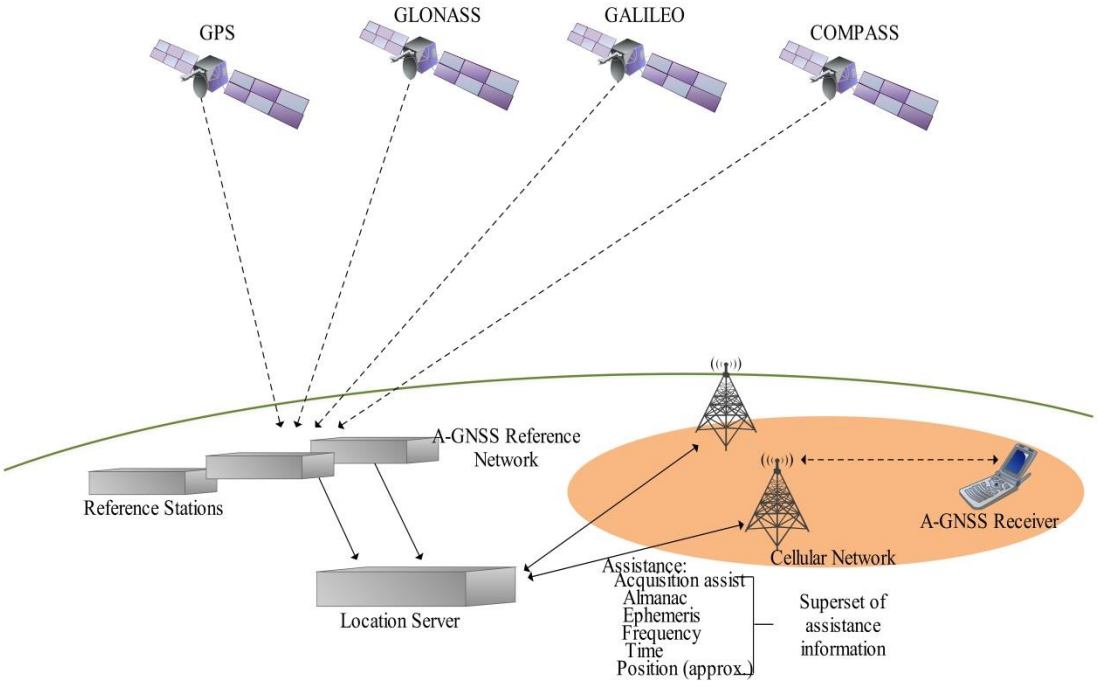


***Figure 1.1.*** *A GNSS overview – system representation [28].*

The frequency of the signal received by the receiver is not exactly same that is transmitted by the satellite transmitter. It is due to the Doppler shift caused by the satellite motion and the receiver motion as well as due to any frequency offset in the receiver oscillator. A receiver with no prior knowledge of these frequency variables needs to search a large range of frequencies. However, even if the receiver acquires the correct frequency, it must still find the correct code delay in order to estimate the TOA of the signal. This is based on finding the correlation peaks from the correlation between the incoming signal and the reference code. Thus, each satellite has a two-dimensional search space.

Figure 1.2 presents an example of a two-dimensional search space. The carrier frequency is search in pre-defined frequency bins and the code-phase of the satellite.

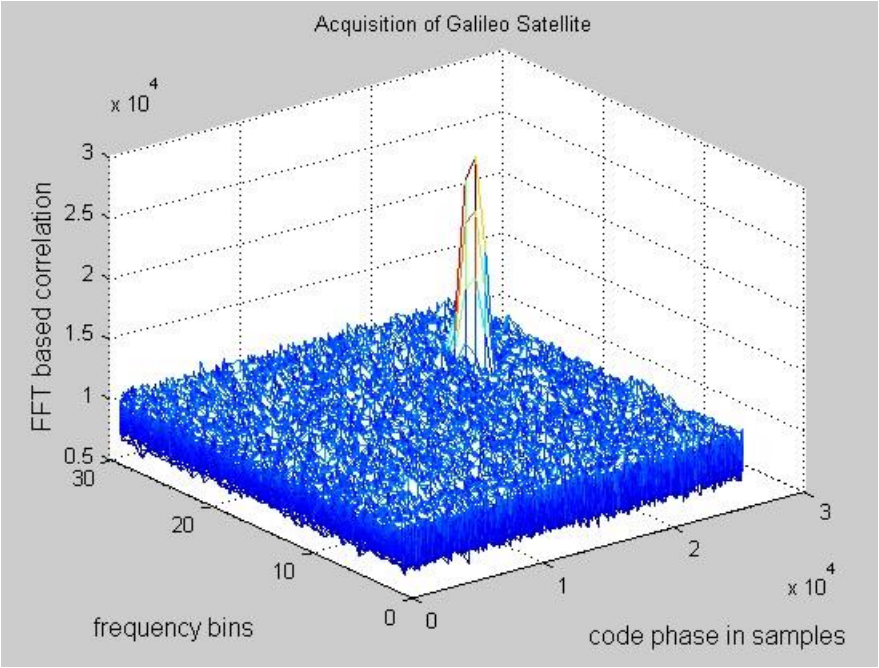


***Figure 1.2.*** *An example of acquisition showing two dimensional search space*

The receiver requires at least 20s to search this search space [28]. Once the correlation peak has been found for each satellite, the receiver needs to decode the navigation data message (i.e., the broadcast time and ephemeris data) which takes about 30s without assistance. Thus, the total time-to-fix (TTTF) is approximately 1 min. Moreover, if the signal is blocked during this time, then the data bit errors may occur, and the receivers will have to wait another 30s for the data to be retransmitted. Thus, conventional receivers take several minutes to get a first fix in a weak-signal environment. The A-GNSS provides the ephemeris data to the receiver so that the receiver does not have to decode the broadcast ephemeris. As a result, time to fix would be reduced by at least 30s. Similarly, A-GNSS provides a rough prior position and prior time to minimize the frequency search and good prior position and a prior time to reduce the code-delay search.

There are two major approaches to A-GNSS known as MS-assisted and MS-based GNSS where "MS" stands for mobile station (GNSS receiver). In MS-assisted GNSS, the position is calculated at a server, and the task of receiver is only to acquire the signals and send the measurements to the server. In MS-based GNSS, the position is calculated by the receiver itself [2; 28].

In the indoor environment, satellite signal becomes weak due to signal attenuation from walls and other obstacles. Similarly, in dense urban environments, there is high attenuation due to obstructions through buildings and multipath reflections. The attenuation on GNSS signal can be up to 20 – 30 dB depending on the electrical properties of building materials. Moreover, the signal suffers from several multipath and NLOS conditions. These limitations of signal propagation in indoor is overcome by high sensitivity GNSS receivers [29]. The high sensitivity receivers usually make use of A-GNSS for position determination. This receiver applies the technique of joint use of coherent cor-

relation and non-coherent integration. The traditional GPS receiver typically uses 1 ms coherent integration time, corresponding to one GPS C/A- code length. The high sensitivity receiver processes a longer period of signals, up to 20 ms coherent integration, corresponding to the length of one GPS navigation data bit. By additionally using long non-coherent integration, they can achieve high sensitivity and avoid the effect of bit transitions and clock drift [30].

## 1.3. Augmentation systems

Augmentation refers to the provision of additional information to enhance the performance of space-based positioning, navigation, and timing signals [5]. Augmentation systems were introduced to meet the real-time integrity monitoring capability required by the civil aviation navigation safety needs, which is the limitation of current GNSS [2]. Augmentations can be space-based, such as a geostationary satellite overlay service or they can be ground-based.

A Satellite-based Augmentation System (SBAS) is a civil aviation safety-critical system that supports wide-area or regional augmentation through the use of geostationary (GEO) satellites which broadcast the augmentation information [2]. The SBAS use a network of terrestrial monitoring stations to perform GNSS ranging measurement. The observations are forwarded to the processing facilities. Using this measurement, the master stations generate correction parameters for the satellite orbits, the satellite clocks, and the ionospheric influence. The SBAS architecture consists of:

- A space segment that consists of the geostationary satellites (GEO) with navigation payloads that transmits GPS-like carrier signal containing SBAS information.
- A ground segment that consists monitoring station network, processing facility center, GEO satellite control center, and communication layer. Ground segment generates and uplinks the augmentation signal broadcasted by the GEO satellite.
- A support segment that consists of all the elements needed to support the correct operation and maintenance of the SBAS
- A user segment that consists of all the user equipment needed to receive and use the SBAS information.

Currently, several SBAS systems are in operational capability, such as Wide Area Augmentation System (WAAS) in United States, European Geostationary Navigation Overlay Service (EGNOS) in Europe, Multi-functional Satellite Augmentation System (MSAS) in Japan, System for Differential Corrections and Monitoring (SDCM) in Russia Federation, GPS Aided Geo Augmented Navigation/GPS and Geo Augmented Navigation System (GAGAN) in India and Satellite Navigation Augmentation System (SNAS) in China.

### 1.3.1. WAAS

WAAS states for Wide Area Augmentation System. WAAS is an extremely accurate United States Satellite-based Augmentation System, started in 1992 and developed by Federal Aviation Agency (FAA) for civil aviation. WAAS was declared operational in the late 2003. The objectives of WAAS are to provide improved integrity, accuracy, availability, and continuity of service to the GPS. The correction improves the accuracy of the system from ten or more meters to just one or two [52]. The WAAS architecture consists of 38 wide-area reference stations (WRS). WAAS coverage was expanded into Canada and Mexico. The expansion was achieved by the integration of nine new international WRS into the WAAS network [15].

### 1.3.2. EGNOS

EGNOS, the European Geostationary Navigation Overlay Service, is the first step on the European contribution to the GNSS, and a fundamental step towards Galileo [53]. EGNOS is an augmentation system to the GPS and GLONASS systems, which provides and guarantees navigation signals for aeronautical, maritime and land applications. It consists of 3 geostationary satellites and a network of ground stations. The initial operational capability of EGNOS was declared in July 2005. It supports all the Galileo services except safety-of-life applications.

### 1.3.3. MSAS

MSAS is the Japanese SBAS, also with the objective to improve the accuracy, integrity, and availability of GPS navigation system. MSAS is a payload of the multifunctional transport satellites (MTSAT) [5]. MSAS is owned and operated by the Japanese Ministry of Land, Infrastructure, Transport, and Tourism and the Japan Meteorological Agency (JMA). MSAS is operational since 2007 and used for supporting en-route, terminal and non-precision approach operations.

### 1.3.4. GAGAN

GAGAN is the Indian SBAS developed in August 2001 by the Indian Space Research Organization in collaboration with the Airports Authority of India. GAGAN provides higher accuracy, integrity, continuity, and availability for Indian Regional Navigational Satellite System. GAGAN improves availability of navigation routes, enabling safe reduction in aircraft spacing. GAGAN signal is compatible with non-aviation receivers with applications to farming, surveying and vehicle navigation.

### 1.3.5. SDCM

SDCM was launched by the Russian Federal Space Agency. SDCM provides integrity monitoring of GPS as well as of GLONASS, unlike other discussed SBAS. SDCM provides differential corrections to GLONASS satellites and a detail analysis of GLONASS system performances.

### 1.3.6. SNAS

SNAS is developed by the People's Republic of China. SNAS is proposed to be implemented in the Chinese Beidou satellite navigation system, using the communication channel for augmentation information transmission [49].

## 1.4. Motivation for satellite-based positioning

Satellite-based navigation is a leading-edge technology that is growing rapidly. Satellite positioning is now an essential tool for all means of navigation. It allows users to identify their locations at any given moment. Until now, GNSS users around the world are dependent on American GPS or Russian GLONASS signals. Galileo gives users a new and reliable alternative under civilian control but not military authorities, nevertheless Galileo is interoperable with GPS and GLONASS. During its initial phase, the first two Galileo Satellites were launched into the first orbital plane on 21 October 2011, followed by another two in a second orbital plane on 12 October 2012, by the Russian Soyuz rocket in French Guiana. These satellites and the future satellites will carry the search and rescue system and payload that were not available in GPS and GLONASS. This search and rescue payload has faster emergency rescue system which helps to save life in emergency. The Galileo satellites are capable of transmitting navigation signal with navigation accuracy and performance in order of magnitude better than any other operational satellites so far today.

Satellite-based positioning provides wide variety of applications in different sectors such as personal application, road application, aviation application, rail application, maritime application, industry application, and so on. Some of the applications of satellite-based positioning are explained below:

- The availability of inexpensive receivers allows the integration of GNSS receivers in different customer products such as in mobile phones. Thus, pedestrian users can easily navigate, determine the current position and find the desired location.
- Satellite receivers installed in vehicles provide services such as real-time traffic information, emergency calls, route guidance, fleet management and advanced driving assistant system. Similarly, it helps to minimize traffic jams.

- The augmentation system gives guaranteed service with sufficient level of accuracy. It helps pilots to assist in all flight phases, from taxing, to take-off, en-route flying, and landing in all weather conditions.
- Satellite-based positioning is very effective in maritime activities such as fishing, oceanography and oil and gas exploitation. Similarly, satellite-based positioning helps in observing the changes of sea level, wrecks location, search and rescue of sinking vessel, dynamic positions and fixing of satellite sea launch platforms.

However, satellite-based positioning is generally not suitable to establish indoor locations. It is because microwaves are attenuated and scattered by roofs, walls and other objects. To overcome this issue, GNSS is integrated with indoor positioning systems.

Taking into account the progress of navigation system in various sectors, this Thesis is focused on one Galileo signal component referred to as Galileo E5a signal. A software receiver will be designed with the help of Matlab Simulator which processes the real-time Galileo E5a signal to determine the exact user location.

## 1.5. Thesis Contributions

The main thesis contributions have been:

- Literature studies and overview of GNSS receivers, in particular the Galileo receivers
- Implementation of a Matlab-based software acquisition unit for Galileo E5a and E5b signals
- Testing and validation of the created acquisition unit with simulated data visa multipath channels, created with an available Simulink E1-E5 model at TUT
- Testing and validation of the software acquisition unit with real-field data collected from Galileo E5b signals (real-field data was provided by FGI)
- Initial testing and loop optimization for a software tracking unit for Galileo E5a signals, including a Delay Locked Lop (DLL) and a Phase Locked Loop (PLL)

The thesis is structured in the following manner:

**Chapter 2** describes the underlying positioning technologies in GNSS, as well as the open challenges of satellite positioning in indoor as well as outdoor environments.

**Chapter 3** gives an overview of GNSS receiver operations.

**Chapter 4** provides the Galileo physical layer specifications as well as briefly describes different kinds of modulations employed in Galileo.

**Chapter 5** discusses the work overflow of the GNSS receiver used in this Thesis.

**Chapter 6** presents the simulation results.

Finally, **Chapter 7** draws conclusions from this thesis work and presents suggestions for future works.

# 2. UNDERLYING POSITIONING TECHNOLOGIES IN GNSS

## 2.1. Time of Arrival (TOA)

The main goal of the GNSS is to provide the user with necessary information to calculate their position. The GNSS utilizes the concept of Time of Arrival (TOA) ranging to determine the user position [2;26]. The principle of TOA is based on measuring the absolute travel time of a signal between the satellite transmitter and the receiver. This time is then multiplied by the speed of the signal equals to the speed of light ($3*10^8\ {}^{m}/_{s}$) in order to obtain the transmitter to receiver distance. If the receiver clock and the satellite transmitter clock are with an offset, the receiver needs to compute an additional distance related to the clock offset [35].

## 2.2. Pseudorange Calculation

The user location can be determined by measuring the propagation time of the signal broadcast from four satellites whose locations are precisely known [2]. If the receiver clock were synchronized with the satellite clocks, only three range measurements would be required. However, a receiver clock always has some offset with respect to the satellite clock because such a crystal clock employed in the receiver has lower stability than the clocks on-board the Thus, four measurements are required to determine user latitude, longitude, height, and the receiver clock offset from internal system time. If either the system time or height is accurately known, less than four satellites are required [2]. The process of determining the user position, velocity, and Time (PVT) by the applying the method of TOA measurement is referred to as trilateration. The idea of trilateration is explained in the Figure 2.1.

The range determined by the correlation process is denoted as the pseudorange $\rho$. The measurement is called *pseudorange* because it is the range determined by multiplying the signal propagation velocity, *c*, by the time difference between two non-synchronized clocks (the satellite clock and the receiver clock).

Figure 2.1 presents a geometry which consists of four satellites in view broadcasting ranging signals. The satellites continuously transmit their positions (i.e. $(x_k, y_{k,} z_k)$, where $x_k, y_{k,}\ and\ z_k$ are the latitude, longitude, and altitude of the *k-th* satellite), keeping their clocks synchronized to a common time scale. With the concept of TOA, distance of each visible satellite is obtained. With the measured distances, circles are drawn around each satellite transmitter with the radius equal to the measured distance.

The receiver is at the position $(x_u, y_u, z_u)$ where $x_u, y_u,$ *and* $z_u$ are the latitude, longitude, and altitude of the user. This receiver is at the position where circles from each transmitter coincide. With the three satellite transmitters, the technique is called trilateration [29].

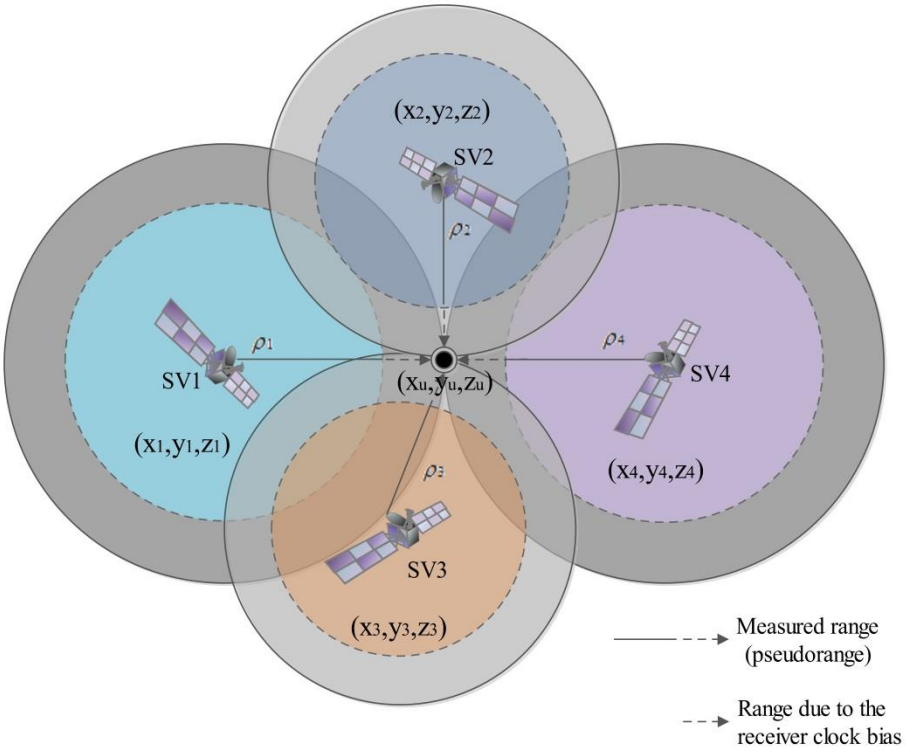


***Figure 2.1.*** *Example of trilateration (reproduced from [58]).*

In order to determine user position in three dimensions $(x_u y_u z_u)$ and the clock offset between the satellite and the receiver, $\delta$, pseudorange measurements are made to four satellites resulting in the system of equations

$$\begin{aligned} \rho_1 &= \sqrt{(x_1 - x_u)^2 + (y_1 - y_u)^2 + (z_1 - z_u)^2} + \delta t * c \\ \rho_2 &= \sqrt{(x_2 - x_u)^2 + (y_2 - y_u)^2 + (z_2 - z_u)^2} + \delta t * c \\ \rho_3 &= \sqrt{(x_3 - x_u)^2 + (y_3 - y_u)^2 + (z_3 - z_u)^2} + \delta t * c \\ \rho_4 &= \sqrt{(x_4 - x_u)^2 + (y_4 - y_u)^2 + (z_4 - z_u)^2} + \delta t * c \end{aligned} \tag{2.1}$$

## 2.3. Open challenges

Determining the satellite positioning in the indoor environment is one the great challenge in GNSS system. The presence of various obstacles such as walls, human beings, and other obstacles leads to multipath effects and the satellite signals lose significant power. As a result, the satellite signals are nearly undetectable in such environments. A-GNSS helps to mitigate to a certain extent this issue, as discussed in the topic above. Not only indoor, but the signals are also affected in outdoor environments due to inter-

ference, multipath, signal fading due to ionosphere, etc. In the following, some of the challenges in GNSS are described.

### 2.3.1. Radio Frequency Interference (RFI)

As GNSS receivers rely on external Radio Frequency (RF) signals, they are vulnerable to RF interference. This interference may result in degraded navigation accuracy or complete loss of receiver tracking. The GNSS deployed Direct-sequence CDMA (DS-CDMA) technique has high processing gain, thus offers protection against low power RFI. However, the moderate and high power interference makes the signal-to-noise-and-interference-ratio (SNIR) low in the receiver, thus can easily degrade the receiver's performance.

Considering the spectral characteristics, interference is normally classified as either *wideband* or *narrowband*. The narrowband interference has a limited fraction of the bandwidth. The potential narrowband interferences are the spurious emissions and out-of-band emission of many broadcast and communication services, such as mobile stations, broadcast television, Very High Frequency (VHF) and Ultra High Frequency (UHF) transmitters [29]. On the other hand, the wideband interference contains energy on the whole radio link bandwidth. Potential sources of interference include Ultra-wide Band (UWB) transmission, inter-system interferences between GNSS systems and intra-system interference between signals of in the same system sharing the same bands [2; 29].

The interference can be intentional if the interference signal is designed to degrade the performance of GNSS receiver. According to the American Volpe National Transportation System Center, the intentional interference can be classified as [29; 34; 59],

- *Jamming,* where a high-power interference signal is transmitted that cause the receiver not to able to detect the navigation signal.
- *Spoofing,* that refers to broadcast of false GNSS signals to produce a false position within the receiver
- *Meaconing,* which is the interception and re-broadcasting of navigation signals in order to confuse navigation timing.

One of the most powerful technologies against radio interference mitigation in GNSS receiver is the multi-element antenna arrays with adaptive beam-forming and null-steering capabilities. However, this technology has the disadvantages of complex hardware, large scale and high cost [29]. Frequency excision technique is another approach to mitigate interference, especially narrowband interference. In this technique, the data samples are converted to frequency domain. The interferences are detected and then reduced to the thermal noise level by comparing the magnitude of each frequency component with a pre-defined threshold [2].

### 2.3.2. Multipath

Multipath propagation is one of the main error sources in GNSS [2; 29]. Multipath is the reception of reflected or diffracted replicas of the signal. As the reflected replicas takes more time to travel to the receiver than the direct path, multipath arrivals are delayed relative to the direct path. As the receiver receives direct signals earlier than the multipath, the receiver can readily resolve them [2]. Thus, such resolvable multipath has little effect on performance. However, multipath signals from nearby objects can arrive at short delays (e.g., tens or hundreds of nanoseconds) after the arrival of the direct path. Such multipath distorts the correlation function between received signal (direct and multipath) and the locally generated reference in the receiver. They also distort the phase of the received signal, introducing errors in pseudorange and carrier phase measurements. It leads to error in measuring position, velocity, and time [2].

Several approaches have been implemented in the last few decades to reduce the multipath effect on a GNSS receiver [29]. Among them, the most important approaches are the use of special multipath limiting antennas (choke ring or multi-beam antennas), the post-processing techniques to reduce carrier multipath, the carrier smoothing to reduce code multipath, and the code tracking algorithms based on receiver internal correlation technique [31; 60]. The use of special multipath limiting antenna may need extra hardware cost, and the post-processing techniques cannot be utilized in real-time positioning. The classical correlation-based code tracking structure is based on a feedback delay estimator also known as Early-Minus-Late (EML) technique [29]. In the classical EML, the early-late correlators are spaced at one chip and fail to cope with the multipath propagation. Thus, a number of enhanced EML techniques have been introduced to mitigate the impact of multipath. One of these enhanced EML techniques is based on the idea of narrowing the spacing between the early and late correlators, i.e., nEML or Narrow Correlator [29; 31]. A correlator spacing in the range of 0.05 to 0.2 chips is commercially available for the nEML-based GPS receivers [31]. Different classes of enhanced EML to mitigate multipath are described in [31; 32; 55-57].

### 2.3.3. Ionospheric Effect

Among the various error sources present in GNSS, ionospheric effect is considered as the biggest part which needs to be estimated and removed [2]. Typically, the ionosphere layer is considered to start at 50 km from the earth surface and to end at 1000 km. It contains charged particles (electrons and ions) which makes ionosphere a dispersive medium. When the signal travels through ionosphere, its velocity changes due to the interaction with particles present in it. Thus, signals transmitted at different carrier frequencies have different phase advances and time delays. This phenomenon leads to a receiver being unable to track one or more visible satellites for short periods of time.

The ionospheric delay depends mainly on two parameters: the total electron content (TEC) and the carrier frequency [33]. As the carrier frequency is a known constant, the

total electron content needs to be estimated in order to further estimate the ionospheric delay. The density of the ionized particles is not uniform in ionosphere. Appleton and Lassen have derived a formula for computing the ionospheric refractive index, with which the ionospheric delay effect can be defined [33]. This effect is a function of the total electron content. Thus, ionospheric effect is mitigated by estimating TEC.

The ionospheric delay mitigation can be categorized depending on the receiver type: single frequency and dual-frequency [33]. In the single frequency receivers, the unknown TEC is found with the help of an appropriately chosen model. Such model shows the ionosphere status for different locations at different time periods. Similarly, these models are responsible for making the necessary corrections for the ionospheric delay. Such model has been proposed for the Galileo-enabled receivers [29; 33]. In the dual-frequency a receiver, modeling of the ionosphere is not required [33] which is one of the main advantages over single frequency receivers. For example, a dual-frequency receiver measures the pseudorange for each of the signals at different frequencies. If both of the pseudoranges are contaminated by the same ionospheric effect, proper combination of the available measurements allows the receiver to completely remove the first order ionospheric effect [29]. The ionosphere delay algorithms for estimation of the pseudorange are presented in [33]. Nevertheless, in the presence of multipath errors, the dual-frequency ionosphere correction algorithms may suffer of limited performance [21; 41].

# 3. GNSS RECEIVERS

GNSS receivers process the signals broadcasted by the satellites in order to determine the position, velocity and precise time (PVT). As the satellites are always in motion, the receivers need to continuously acquire and track the signals from the satellite in sight, to provide an uninterrupted solution. Figure 3.1 shows the block diagram of general GNSS receiver. It is composed of the Radio Frequency (RF) Front end, the digital signal processor (DSP), and the navigation processor. The signals transmitted from the satellites are first received by receiver's antenna. Through the front-end, the input signal is amplified and down-converted to the desired frequency and further digitized by ADC for further basedband processing. The digital signal processor is the main focus of this thesis. In DSP, the presence of the signal is detected by an acquisition method. When the signal is acquired, the signal is passed to tracking process. The tracking process follows continuously the code and carrier parameters of the incoming signal and thus accurately extract the navigation data. The navigation processor provides the complete navigation solution giving position, velocity, and time of the user. The detailed description of each block is presented below.

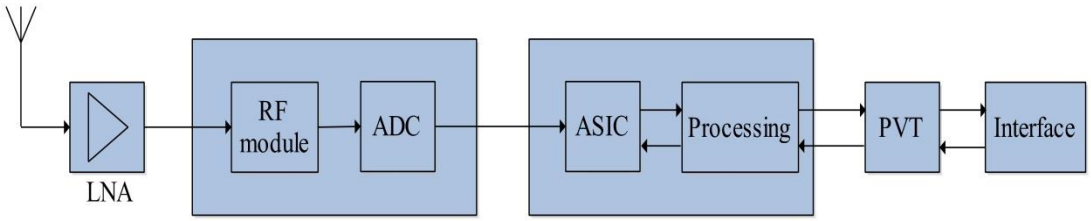


***Figure 3.1.*** *A basic block diagram of general GNSS receiver*

## 3.1. Front End

The antenna is the entry point of the front end. It is the main interface between GNSS Space Segment and the User Segment. It receives L-Band signals (1.2 -1.6 GHz range RF signal), pre-processes and passes to the RF front end. The main objective of antenna is to maximize the antenna gain towards the emitting satellites while rejecting multipath signals and interference. The incoming satellite signals from the antenna are filtered and amplified. The signals are then downconverted to an Intermediate Frequency (IF) using a frequency mixer and then, they are filtered again for image rejection and additional out-of-band signal rejection. High-power signal parts are normalized by the automatic gain control (AGC) and are sampled by analog to digital converter (ADC). The sampled

signals are then passed to a digital signal processor (DSP). Figure 3.2 illustrates the general block diagram of RF front end.

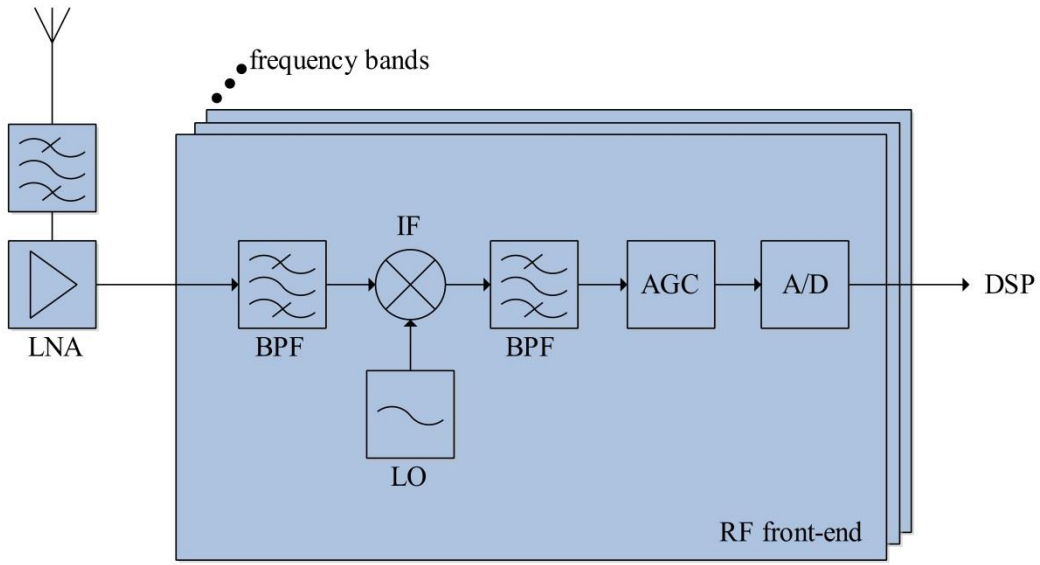


***Figure 3.2.*** *Generic radio frequency front-end functional block diagram (reproduced from [5]).*

### 3.1.1. Filtering and amplification

The filtering stages are necessary to ensure a low noise and out-of-band rejection in the received signals. An out-of-band interferer is an RF source outside of the GNSS frequency bands, which may cause the low noise amplifier (LNA) to go to nonlinear range. It is prevented by filtering [5].

Amplification is performed to compensate transmission losses. The signals received from antenna are very weak. Moreover, the cable and the receiver elements also generate some noise. To minimize the overall noise figure, LNA is added in the front-end chain [5].

### 3.1.2. Mixer/Local Oscillator

The combination of the mixer and the local oscillator downconverts the input RF carrier to a lower intermediate frequency (IF) and preserve the modulated signal structure. The downconversion is performed in order to bring the frequency of signal to a usable range so that it is easy to operate maintaining the quality and minimizing the cost of the receiver component [3]. The process of mixing is accomplished by multiplying the incoming RF signal centered on the frequency $f_r$ with a locally generated pure harmonic signal $f_l$. The local oscillator (LO) is typically a combination of components. It is because most standalone or temperature-compensated quartz local crystal oscillators cannot generate the desired local oscillator frequency for the GNSS signal. Furthermore, the reference oscillators should have low sensitivity to vibration and have low phase noise.

Thus, a phase lock loop (PLL) is combined with the crystal to achieve the desired higher frequency of the LO [3; 10].

The mixer operates through the trigonometric identity expressed as [5]

$$\cos(2\pi f_r t)\cos(2\pi f_l t) = \frac{1}{2}\cos(2\pi(f_r + f_l)t) + \frac{1}{2}\cos(2\pi(f_r - f_l)t) \quad (3.1)$$

The term $f_{IF} = f_r - f_l$ is referred to as intermediate frequency (IF), which is the downconverted part of the signal. The higher frequency part, $f_r + f_l$, is filtered using a band pass filter. Although the mixing process shifts the frequencies in the electromagnetic spectrum, it does not affect the phase shift and Doppler shifts in the code sequence, because the mixing is a linear operation [5].

### 3.1.3. Analog-to-Digital Converter

The analog-to-digital converter (ADC) is the final component in the front-end chain. This device converts analog signal to digital samples. The key parameters to be considered in ADC are the number of bits, the maximum sampling frequency, the analog input bandwidth, and the analog input range.

One bit quantization is generally sufficient for signal acquisition and tracking in mass-market receivers. However, higher quantization levels (e.g.: 2-bit or 4-bit) show a better signal-to-noise ratio and decrease susceptibility to interference. Ideally, the signal distortion of a 1-bit quantization is less than 2 dB and of 2-bit or more quantization is less than 1 dB [3; 5].

The maximum sampling frequency is chosen such that it needs to cover the bandwidth of the desired signal. The sampling frequency is chosen by the Nyquist (Shannon) theorem as the sampling frequency should be atleast greater than twice the one-sided baseband bandwidth. Typically, sampling rates of 2 to 20 times the PRN code chipping rate are used [5].

The analog input range describes the voltage range for which the quantization will be distributed across [3]. Assuming a 50Ω load, a 1 Volt peak-to-peak input corresponds to -17 dBW. The input level contains thermal noise. Thus, amplification is necessary to amplify the input so that ADC can process the input.

### 3.1.4. Automatic Gain Control

The automatic gain control (AGC) is an amplifier which acts as a feedback loop that controls the power levels of the received signal. It has a variable gain with a feedback signal resulting from processing implemented after the ADC. The objective of front end is to process all the bits with the ADC. AGC maintains and controls this objective such that the gain of input signal to ADC is neither too low nor too high. The sampled received from front end is passed to the digital signal processor (DSP) for the acquisition and tracking process. AGC can be also used to detect narrowband interferers.

## 3.2. Digital Signal Processor

The digital signal processor (DSP) process the downconverted and digitized GNSS signal and provides code pseudoranges and carrier phase measurements, as well as navigation data. The signal is first split into number of channels that track each satellite signal separately. Then, the information from each channel is integrated to find a navigation solution. Before assigning the channel to a satellite, receiver must identify initially visible satellites which can be done either by *cold start*, *warm start* or *hot start*.

In a **cold start**, the receiver has no prior information about its own position or which satellites are in view. Thus, the receiver starts from scratch searching for satellites instead of relying on any stored information. As a consequence, each channel has to perform extensive search of all possible signals. The method is referred to as acquisition [3].

In a **warm start**, the receiver has access to its last position before powering down the receiver. The receiver combines this information with the information in the stored almanac data and gives rough position of all satellites at the real time. Thus, receiver determines which satellite is visible, and estimates their rough code delay and Doppler frequency, hence being able to narrow down the acquisition search space. However, If the receiver is moved to the different location since it was switched off, then the receiver position cannot be trusted and the satellites found do not match with the actual visible satellites.

In a **hot start**, the receiver has access not only to its rough initial position, but also to the ephemerides of the satellites. Thus, this process greatly reduces the acquisition search space, which improves the time to acquire and therefore the final time to first fix (TTFF).

Figure 3.3 gives an overview of one receiver channel. The following section describes each block in detail.

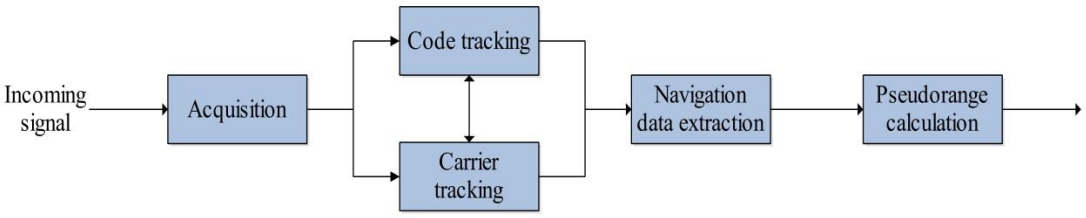


***Figure 3.3.*** *A generic signal processor functional block diagram (reproduced from [3]).*

### 3.2.1. Acquisition

The objective of the acquisition stage is to identify all the visible satellites and the coarse values of carrier frequency and code phase of the satellite signal. The carrier frequency is the downconverted satellite signals to IF frequency. The frequency of the signal from a specific satellite can be different from its nominal value. It is due to relative

motion of the satellite with respect to the receiver causing Doppler Effect [3]. The code phase refers to the time alignment of the PRN code in the current block of data. Acquisition is performed by a correlation between the incoming signal and a reference code at the receiver.

The idea of correlation is, when the code is correlated with an aligned replica of itself, the correlation output is maximum, referred to as high auto-correlation. Similarly, when the code is correlated with a non-aligned replica of itself, then the output is low. And when the code is correlated with another code of the same family, the correlation output is low, referred to as low cross-correlation.

The received signal $s$ in a DSP channel is a combination of signals from all $N$ visible satellites. These signals are the mixture of multipath signals, interference, and noises. When acquiring the satellite $k$, the received signal $s$ is multiplied with the locally generated PRN code that is replica of satellite $k$. The local replica of PRN code is generated in such a way that it must have the correct code phase to that of the corresponding satellite. Thus, the presence of satellite signals is found through correlation between the incoming signal and each satellite PRN code with different delays and frequencies. A high enough correlation peak indicates the visibility of the corresponding satellite at a coarse delay estimate and a coarse frequency estimate.

The coarse frequency and code delay can then be estimated. To determine the frequency and code delay, a search space is defined. The search space must cover the full range of uncertain code delay and frequency. Thus, it equals to the length of spreading code, for example, 10230 chips for Galileo E5 signal. The resolution of the code bin is number of samples according to the sampling frequency of the receiver. The frequency of the locally generated signal must be close to the signal carrier frequency. The frequency of the received signal can vary up to ±10 kHz from the nominal frequency, so different frequencies within this range must be tested. In [3], the authors stated that inorder to check the visible satellite it is sufficient to search the frequency in steps of 500 Hz that results in 41 different frequencies in case of fast-moving receiver and 21 in case of a static receiver.

After mixing with locally generated carrier wave, the signal components are squared and added. The output is a value of correlation between the incoming signal and the locally generated signal. If the output exceeds a predefined threshold, the visible satellite is acquired and it can be tracked. Figure 3.4 shows a typical acquisition plot of the Galileo satellites. Figure 3.4a is the output of an acquisition plot performed for a visible satellite. The plot shows a significant peak, which indicates high correlation. Similarly, Figure 3.4b is the output of an acquisition plot performed for a satellite that is not currently visible to the Galileo receiver. In this plot, all values are nearly identical, indicating low correlation.

Depending on several search techniques, a search space can be divided into several search windows. Three are three different methods to implement acquisition in a software receiver. They are serial search acquisition, parallel frequency space search acquisition, and parallel code phase search acquisition.

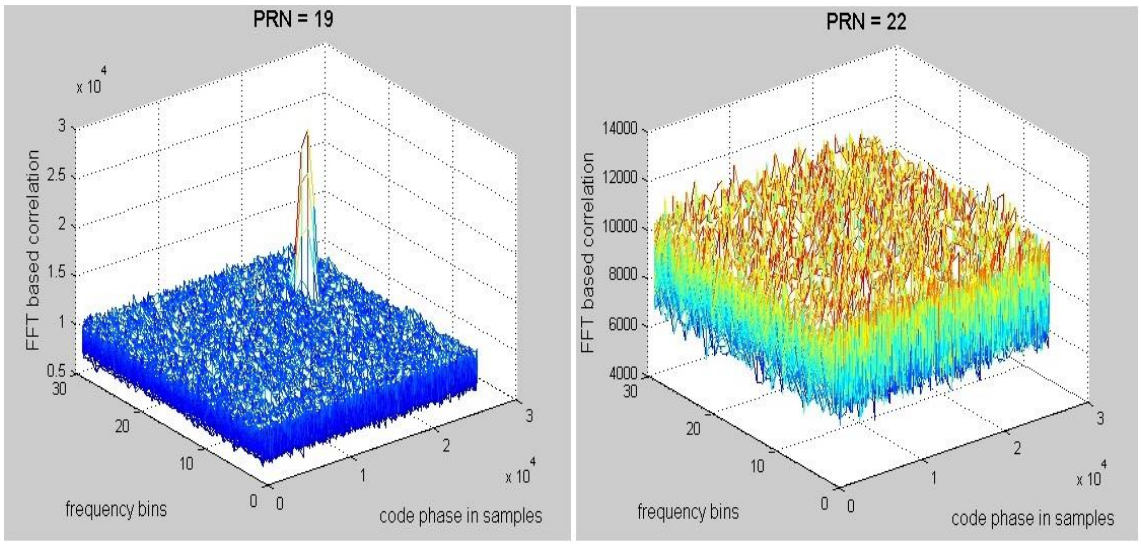


(a) (b)

***Figure 3.4.*** *(a) Acquisition plot for PRN 19, (b) Acquisition plot for PRN 22.*

In serial search acquisition, search is performed over all possible carrier frequencies of IF±10 KHz and a code phase over all 10230 codes (in case of Galileo E5 signal). Thus, the serial search method is a very time-consuming procedure. The parallel frequency space search acquisition parallelizes the frequency space search. That is, this method performs the search only through different code phases thus this method is a faster implementation as compared to the serial search acquisition. The parallel code phase search acquisition parallelizes the code phase search. That is, the search is performed only in the defined frequency steps as compared to the 10230 code phase (in case of Galileo E5 signals). Thus, this method of acquisition is faster as the search space is minimized from large code steps to few frequency steps.

### 3.2.2. Tracking

The acquisition provides only some rough estimates of the frequency and code phase parameters. The objective of the tracking stage is to refine these values, to keep track of the satellite, and demodulate the navigation data from the particular satellite. Tracking module generates two replicas, one for carrier and one for code to perfectly track and demodulate the signal of one satellite.

#### 3.2.2.1 Code Tracking

The code tracking loop keeps track of the code phase of specific code in the signal such that the output generated is the perfect aligned replica of the code. A delay lock loop (DLL) referred to as an early-late tracking loop is typically used as a code tracking loop. In DLL, three local replicas are generated and correlated with the incoming signal. These replicas are referred to as the early, prompt, and late replica, respectively. These

codes are typically separated by a half-chip length, but narrower spacing is also possible. Figure 3.5 shows a basic block diagram of a code tracking loop.

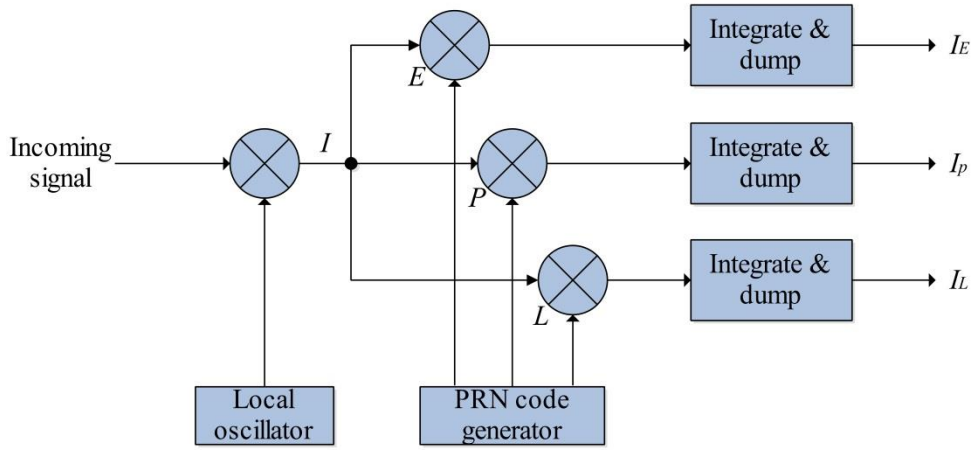


***Figure 3.5.*** *Basic code tracking loop block diagram (reproduced from [3]).*

In Figure 3.5, the incoming signal is mixed with locally generated carrier that shifts the frequency spectrum of the signal to zero frequency. The signal is then multiplied with three code replicas which are early, prompt, and late replicas, and each of these correlations are then integrated and dumped. The output from integration indicates how much the specific code replica correlates with the code in the incoming signal [3].

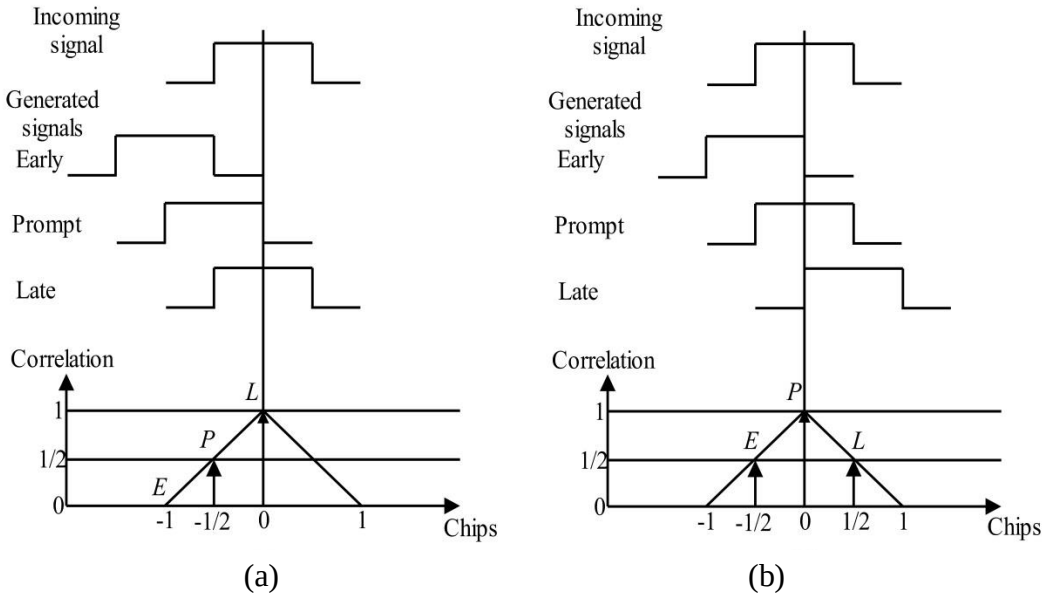


***Figure 3.6.*** *An example of code tracking (reproduced from [3]).*

The three correlation outputs $I_E$, $I_P$, and $I_L$ are compared to see which one provides the highest correlation. If the prompt code has the highest correlation, and the early and late code have similar correlation, then the loop is perfectly tuned in. Figure 3.6 shows an example of code tracking. In Figure 3.6a, the late code has the highest correlation, so the code sequence must be delayed. In Figure 3.6b, the prompt code has the highest cor-

relation, and the early and late replicas have equal correlation. Thus, the code phase is perfectly tracked [3].

The DLL in Figure 3.5 works properly only when the phase and frequency of incoming signal is locked with the locally generated carrier. If the phase and frequency do not match, the integration will decrease as a function of phase shift. To overcome this issue, incoming signal is correlated with two 90º phase shifted locally generated signals. Figure 3.7 shows DLL block diagram with six correlators. In the Figure 3.7, if the local carrier wave is in phase with the input signal, all the energy will be in the in-phase arm. But if the local carrier phase changes compared to the input signal, the energy will switch between the in-phase and quadrature arm.

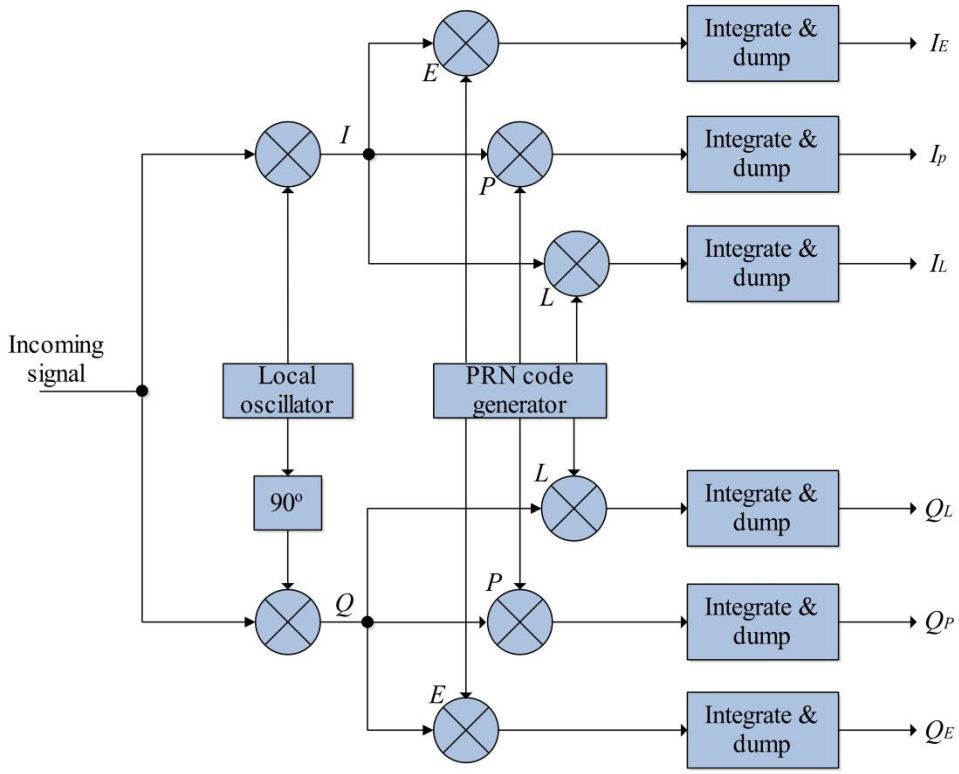


***Figure 3.7.*** *DLL block diagram with six real correlators (or 3 complex correlators) (reproduced from [3]).*

### 3.2.2.2 Carrier Tracking

Carrier tracking demodulates the navigation data successfully by creating a feedback loop that generates an exact carrier wave replica. To track a carrier wave signal, phase lock loops (PLL) or frequency lock loops (FLL) are often used. Figure 3.8 shows a basic block diagram for a phase lock loop.

In the Figure 3.8, the output from the early-late code tracking loop, $I_P$ is the input for the carrier tracking loop. The first two multiplications remove the carrier and the PRN code of the input signal. The carrier loop discriminator finds the phase error on the local carrier wave replica. The output is then filtered and used as a feedback to the nu-

merically controlled oscillator (NCO) until the frequency of local carrier wave and input is not matched.

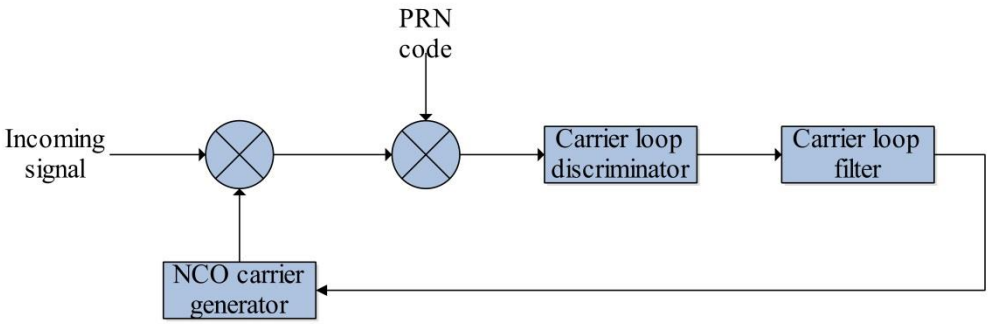


***Figure 3.8.*** *A block diagram of basic GNSS receiver tracking loop (reproduced from [3]).*

There is one drawback of this block diagram. That is, it is sensitive to 180º phase shifts [3]. To mitigate this problem, Costas loop is used for PLL. The objective of Costas loop is to try to retain all the energy in the in-phase arm. The input signal is multiplied by a locally generated carrier wave and 90º phase shift carrier, thus splitting the input signal into the I and Q branches. The high-frequency component from the output is filtered using low pass filter. The signals are then passed through the carrier loop discriminator. The loop discriminator calculates the phase error. The output of the discriminator is filtered in the carrier loop noise filter to predict and estimate any relative motion of the satellite and to estimate the Doppler frequency. The output from the filter is fed as the feedback input. The phase error is minimized when the correlation in the quadrature-phase arm is zero and the correlation in the in-phase arm is maximum. Figure 3.9 shows a basic block diagram for Costas loop.

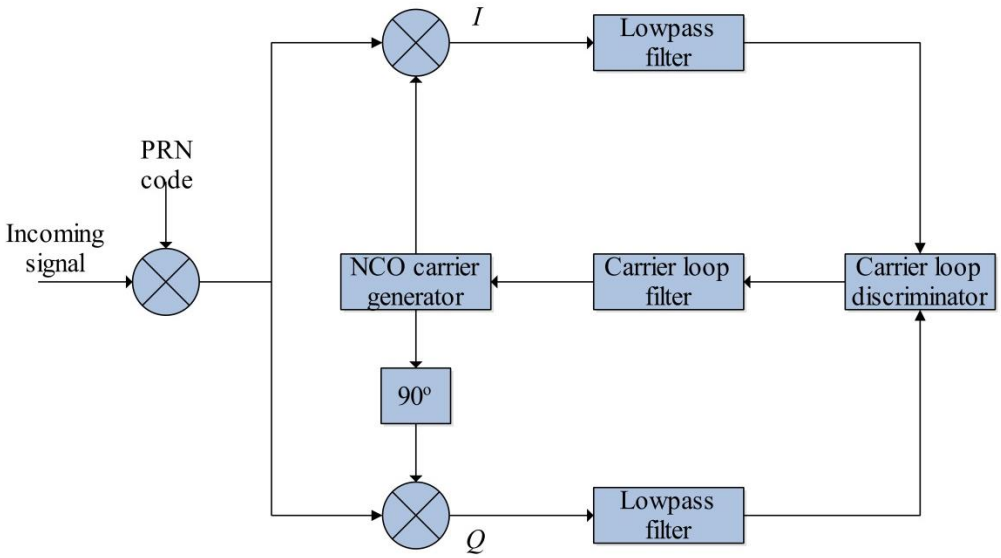


***Figure 3.9.*** *Costas loop used to track the carrier wave (reproduced from [3]).*

The tracking is running constantly to track the changes in frequency as a function of time. If the receiver loses track of a satellite, a new acquisition must be executed for that particular satellite.

## 3.3. Navigation Data Extraction

The tracking process removes the ranging code and the carrier wave from the signal leaving only the navigation data bits which is either 1 or -1. This output is processed by the navigation processor. The task of navigation processor includes data demodulation which results decoding the navigation message and computing satellite positions. Similarly, navigation processor calculates position, velocity, and time information. The third task includes providing aiding information to the tracking loops and to the filters. Figure 3.10 shows the basic data demodulation scheme that demodulates the input signal and obtains the navigation message.

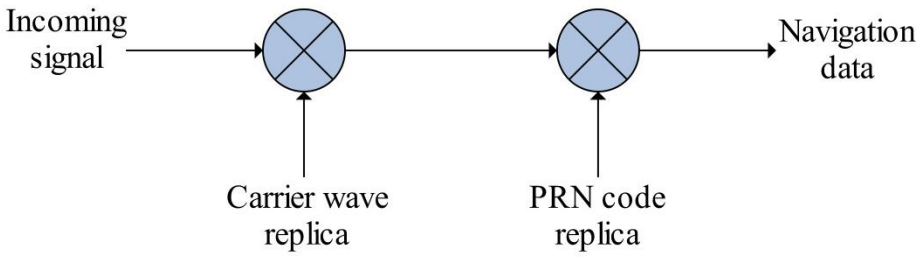


***Figure 3.10.*** *Basic data demodulation scheme [3].*

The data demodulation includes bit synchronization, frame synchronization, and message decoding [5]. The navigation data has bit rate of 50 bps whereas the sample rate of the output from the tracking block is 1000 sps. Thus, before the navigation data can be decoded, the signal from the tracking block must be converted to 50 bps. It means, 20 consecutive values are replaced by a single bit. This process of conversion is referred to as bit synchronization. Similarly, frame synchronization consists in identifying beginning of the message subframes. In case of GPS, the navigation message is divided in frames. Each frame is divided into subframes. In case of Galileo, a frame is composed of several subframes, and a subframe, in turn, is composed of several pages [12]. The start of a subframe consists of a sequence of preamble bits, (a page in case of Galileo) [3; 12]. Thus, if the preamble is identified then the beginning of the subframe can be identified. The preamble search is implemented through correlation. The incoming sequence of navigation bits is correlated with the sequence of preamble bits. The correlation output gives maximum correlation where the preamble bits are contained thus identifying the beginning of subframes. When the correct preambles are located, the data from each subframe can be extracted. These data includes orbital parameters necessary to compute the satellite position corresponding to the transmission of the subframe.

The final task required before making position computation is the pseudorange calculation. Pseudorange is the estimated distance between a satellite and a navigation sat-

ellite receiver. It is computed based on the transmission time of signal from the satellite and the time of arrival at the receiver. It is estimated as the multiplication of transmission time from the satellites to the receiver by the speed of the signal. Thus, user position is computed from pseudoranges and the satellites positions obtained from the orbital parameters.

## 3.4. Hardware versus software receivers

A basic block diagram of a conventional hardware GNSS receiver is similar to that shown in Figure 3.1 above. It consists of an antenna linked to a series of application specific integrated circuits (ASICs) that feeds sampled signals into digital correlation chips and controlled by a central processor [11]. In such a receiver, the processor needs to read, interpret, and adjust the inputs and outputs of the signal correlator channels at a fast rate. It is because, huge receiver algorithms are executed in the main processor using register or memory interfaces to the correlation chips. Such a bulk conventional receiver consumes lots of power and cost is high. Moreover, once the receiver is designed, the options in radio frequency (RF) tuning and digital signal processing (DSP) is limited. Thus, to optimize the speed, cost, and power performance of the receiver, a conventional GNSS receiver is modified to either field-programmable gate array (FPGA) technology or a software based receiver in most navigation systems available today.

The FPGA-based receiver has grown popularity significantly due to the integration of high circuit density on a relatively small programmable chip at a low cost [11]. The FPGA chip is programmed in a custom design language known as VHDL. This design language configures the millions of generic circuit gates inside FPGA that performs specified functions. One advantage of the FPGA is that it can perform fast Fourier transform (FFT) that is used more often during a GNSS receiver's initial search and acquisition operations. The FPGA can only be programmed for certain tasks and it is difficult to implement many functions [11]. For example, the FPGA can perform GPS signal tracking but complicated control logic, which is often present in navigation software control architectures, is not effective to perform in FPGA. Thus, a separate control processor is needed to perform it. It is one of the drawbacks of the FPGA. Moreover, FPGA can draw more power than a conventional ASIC hardware.

Software receiver implementations are becoming more and more popular. A software GNSS receiver simplifies the receiver design as it eliminates digital processing hardware. It has capability of reprogramming to work under different standards with minimum hardware change. Similarly, it overcomes the limitation of RF tuning and DSP portion of conventional GNSS receiver [13]. Other advantages of a software receiver over hardware receiver include decreased size, low power consumption, low cost, and flexibility. Moreover, it overcomes the nonlinearity caused by analog components and their temperature-base and age-based characteristics. But, there are also some limitations in a software receiver, such as, the processing load of control processor being increased in the software and the processing time being typically longer than in hard-

ware implementations. The software receivers need to perform a large array of multiplications and accumulations frequently. However, a software receiver can run several channels in parallel in real time. For example, in [14] a demonstration was shown with 12 parallel channels. The following section describes some types of software-defined receiver simulators which can be found nowadays in the research world.

## 3.5. Software GNSS simulators

### 3.5.1. GPS software receiver

A fully-functional GPS software receiver was initiated at Aalborg University in the early spring of 2004. The software development was started as a student project/Master thesis. After completion, it was implemented as GPS L1 software receiver in MATLAB that was capable of computing positions accurate to about 10 meters [3]. The processing of the satellite signals was done off-line (no capabilities of real-time processing). It was designed for the GPS signal and thus had an in-depth knowledge of the GPS signal structure and signal processing algorithms. The receiver algorithms contain GPS signal acquisition, code tracking, carrier tracking, and additional algorithms needed to supply a receiver position once every millisecond. This software receiver has also been the base of the FGI software receiver, which has been the starting point in this thesis. The Aalborg GPS software receiver is freely distributed with [3].

### 3.5.2. NavX®-NSR

NavX®-NSR is the first interactive GPS/Galileo L1/E1 software receiver, introduced by IFEN GmbH [16] in which all signal acquisition, tracking and positioning tasks are performed in software. Similarly, low-level parameters such as number of channels, sample rate or even the PRN codes can be modified by the user. This simulator provides measured pseudorange, carrier phase and instantaneous Doppler shift outputs. The NSR software is composed of processing core, real-time USB IF sample input, IF sample load/save, graphical user interface/configuration manager and application programming interface [16]. In NSR, user can access all the stages of the GNSS receiver. That is, the NSR offers a flexible Application Programming Interface (API) for this purpose thus enabling the user to add, replace, or expand the capabilities of the receiver according to the requirements. The API consists of C-structs and C- functions which are called on loading or leaving the API. The user has to implement these functions in C/C++ as a Dynamic Link Library. These functions are loaded by the NavX®-NSR framework at program runtime [16]. The NSR software offers both, a real-time mode as well as post-processing mode, which is able to work with stored IF sample files.

### 3.5.3. gLab

*gLab* is a proprietary GNSS software receiver developed in various projects by both Italian for the Italian Space Agency (ASI) and European with ESA. It allows the user to generate a fully custom GNSS signal, process them using powerful digital signal analysis capability and analyses the results using a simple user friendly multimedia interface (MMI) [17]. It consists of three separate modules: generation module, processing module and analysis module. These modules are independent and can be configured by the user. Generation module includes generation of all the three Galileo bands (E1, E5, and E6), GPS signals (L5, L2C, and L1C), and the European Augmentation signal EGNOS [17]. The processing module processes and analyzes the real or synthetic data generated from generation module. The task of processing module includes analysis of acquisition and tracking, AltBOC and MBOC performance, PLL/DLL loop design, channel-to-noise estimation, and multipath and interference analysis. Analyzer module extracts navigation message from the GNSS signals after processing from the processing module. *gLab* is implemented in C programming and the MMI is implemented in GIMP Toolkit (GTK+) programming. It runs on a standard PC using Linux operating system. The processing components of gLAB works as an high end GNSS software receiver with possibility to analyze both real data or off-line data, generated with gLAB generation module [17].

### 3.5.4. GRANADA Bit-true Receiver simulator

GRANADA (Galileo Receiver ANAlysis and Design Application) Bit-true software receiver simulator [18] is a Simulink-based acquisition and tracking simulator developed by Deimos Space, for testing the performance of the algorithms applying in the Galileo receiver. It was developed within Galileo Receiver Development Activities (GARDA) project, funded by from European Union, through the Galileo Joint Undertaking (GJU). It is a modular and configurable tool that implements a dual-channel receiver (data and pilot channel). The simulator consists of three blocks: the Galileo transmitter block, the propagation channel block and the Galileo receiver block. The transmitter includes the code generation, BOC modulation, and channel multiplexing. The propagation channel includes the multipath, the Additive White Gaussian Noise (AWGN) and other sources of interference from other satellites. The receiver block implements acquisition and code tracking function [18]. The GRANADA simulator is developed in MATLAB/Simulink and it is not based on real-time processing. It is available for purchase for research and commercial purposes, but many of its source codes are proprietary, meaning that the user does not have much flexibility in changing the existing blocks.

### 3.5.5. Real-Time Dual-Frequency (L1/L5) Software Receiver

A real-time software receiver was developed in [14] that support GPS/WAAS dual-frequency (L1/L5) processing. The software is developed with Visual Studio under Windows. Most of source code is programmed using C++. Similarly, inline assembly is used to program correlation operations having high computational complexity. This receiver is capable of positioning solely on L5 ranging code and can estimate ionosphere delay using L1-L5 measurements, which are the key contributions of the receiver.

### 3.5.6. BaiCES software simulator

BaiCES software simulator was developed within the BaiCES project (2001-2003) in cooperation with the IfEN GmbH and the Astrium EADS GmbH as prime contractor, financed by the BFS (Bayerische Forschungsstiftung). The target of this simulator is to combine all the main aspects of existing GNSS simulation tools of the three projects partners to a big simulation tool. The BaiCES simulator is based on the commercial simulation environment, ML-Designer, from the Mission Level Design GmbH [22; 23]. The simulation is designed graphically, by drag and drop models from the model library into the simulation build up window and connecting the in and out ports. A model library consists of model that represents a certain part of a GNSS system such as the satellite orbit, the satellite signal, the receiver or the user environment.

### 3.5.7. MGOS

MGOS (Multi-GNSS Observables Simulator) is a graphical software simulator developed to generate pseudorange and carrier-phase measurements for the GPS, GLONASS, Galileo, and Compass constellations. Its operation and appearance is similar to the BaiCES software simulator. SATNAV toolbox is used as initial bench mark to design MGOS as this toolbox was developed for the similar purpose [23]. A MGOS consists of two main components: a graphical user interface (GUI) and a module library. With GUI, a user can easily create simulation scenarios. Similarly, a module library consists of satellite, receiver, error source, and data visualization modules [24].

### 3.5.8. GNSS Simulink model at TUT

The Galileo E1 and E5 signal simulators are designed in a Simulink-based platform at Tampere University of Technology (TUT), Finland. The basic simulator version was designed in the early 2009. The model has been extended by adding several signal processing blocks and algorithms, such as multipath mitigation algorithms, and interference and mitigation blocks. Similarly, whole E5a signal acquisition and tracking blocks has been added in the E5 signal simulator. The Galileo E1 and E5 simulators are built within the Galileo Ready Advanced Mass MArket Receiver (GRAMMAR) project and they

are available under open-access license terms for research community [25]. The simulators focus only on acquisition and tracking blocks and offer only off-line signal processing.

The objective of the Simulink model is to simulate the performance of developed link-level algorithms for acquisition and tracking of Galileo signal. The simulator is designed in Simulink tool under MATLAB. It is because Simulink provides an interactive graphical environment and a customizable set of block libraries. Thus, it is easy to design, simulate, implement, and test a variety of time-varying systems. Parts of this simulator have also used for the purpose of this thesis as explained in Section 6.1.

### 3.5.9. FGI-GSRx software GNSS receiver

FGI-GSRx software is the GNSS receiver re-designed by Finnish Geodetic Institute (FGI), Department of Navigation and Positioning, Masala, Finland. which was initiated from the open source GNSS software receiver developed at Danish GPS Centre at Aalborg University for acquisition and tracking of GPS L1 band signal [3]. Finnish Geodetic Institute implemented the software to acquire Galileo E1 band and Beidou B1 band signals including GPS L1 band signals [54]. The FGI-GSRx software Galileo receiver is designed to run in the Graphical User Interface Design Environment (GUIDE) tool in Matlab. This thesis is implemented in FGI-GSRx software GNSS receiver. The goal of the thesis is to extend the software receiver to acquire the real-time Galileo E5a band signals. The detailed description of this software receiver is explained in Chapter 5.

# 4. GALILEO PHYSICAL LAYER SPECIFICATIONS

The Galileo program is Europe's initiative for a state-of-the-art global satellite navigation system, providing a highly accurate, guaranteed global positioning service under civilian control [36]. While providing autonomous navigation and positioning services, the system established under the Galileo program will at the same time be interoperable with other GNSS systems such as GPS and GLONASS. The fully deployed Galileo system will consist of 30 satellites (27 operational and 3 spares), positioned in three circular Medium Earth Orbit planes at a nominal average orbit semi-major axis of 29601.297 Km, and at an inclination of the orbital planes of 56 degrees with reference to the equatorial plane [4].

The Galileo system consists of three independent CDMA signals, named E5, E6, and E1, permanently transmitted by all Galileo satellites. The E5 signal is further subdivided into two signals denoted by E5a and E5b. Figure 4.1 specifies the radio-frequency air interface between the space and user segments.

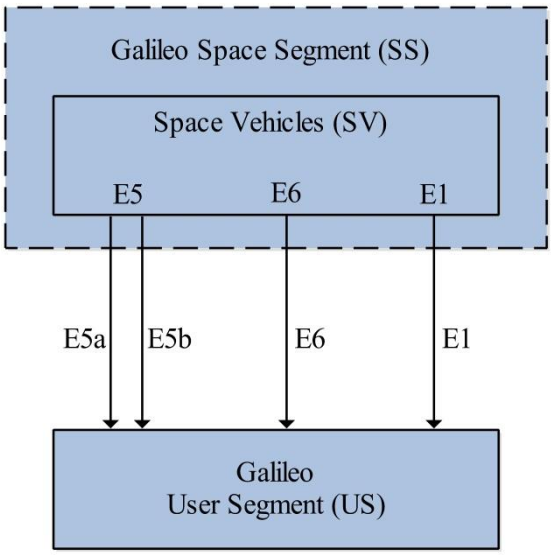


***Figure 4.1.*** *Space Vehicle/Navigation User Interface (reproduced from [4]).*

## 4.1. Frequency Plan

The Galileo navigation signals are transmitted in the four frequency bands E5a, E5b, E6, and E1 bands. They provide a wide bandwidth for the transmission of the Galileo Signals. Figure 4.2 shows the Galileo frequency plan. It can be seen that the Galileo

frequency bands have been selected in the allocated spectrum for Radio Navigation Satellite Services (RNSS). The E5a, E5b, and E1 bands are included in the allocated spectrum for Aeronautical Radio Navigation Services (ARNS), employed by Civil-Aviation users, and allowing dedicated safety-critical applications [4]. As shown in the figure, the Galileo E5a signal shares the same bandwidth with the GPS L5 band. Similarly, the Galileo E1 signal has same carrier frequency with the GPS L1 signal but with slightly wide bandwidth. These two frequency bands, E5a and E1, have been chosen purposely in common to the GPS in order to increase interoperability and compatibility between Galileo and GPS.

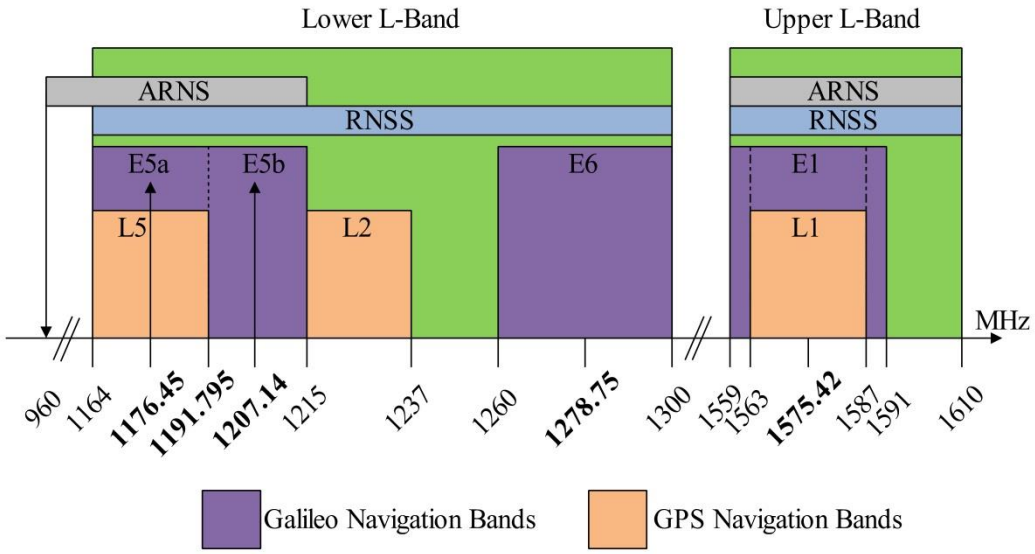


***Figure 4.2.*** *Galileo Frequency Plan (reproduced from [4]).*

Table 4.1 shows the Galileo carrier frequencies and the receiver reference bandwidths centered on their carrier frequencies. As seen from the Figure 4.2 and Table 4.1, the signals E5a and E5b are part of the E5 signal in its full bandwidth.

***Table 4.1.*** *Galileo Frequency per signal and Receiver Reference Bandwidths*

| Signal | Carrier Frequency (MHz) | Receiver reference Bandwidth (MHz) |
|---|---|---|
| **E1** | 1575.420 | 24.552 |
| **E6** | 1278.750 | 40.920 |
| **E5** | 1191.795 | 51.150 |
| **E5a** | 1176.450 | 20.460 |
| **E5b** | 1207.140 | 20.460 |

## 4.2. Galileo Services

The Galileo system is an independent navigation system that aims at providing a number of guaranteed services to users equipped with Galileo-compatible receivers. The

following Galileo satellite-only services will be provided worldwide and independently from other systems by combining Galileo signals-in-space:

### 4.2.1. Galileo Open Service (OS)

The Galileo Open Service provides positioning, velocity, and timing information that can be accessed free of direct user charge. This service is suitable for mass-market applications, such as motor vehicle navigation and location-based mobile telephone services. In general, Open Service applications will use a combination of Galileo and GPS signals. The Galileo OS is accessible through the signals GPS L1, Galileo E5a and E5b, whether data or pilot [47]. The usage of several signals and frequencies increases the performance and interference resistance but at the same time increases technological requirements [5].

### 4.2.2. Galileo Safety of Life (SoL)

The Galileo Safety of Life service improves the Open Service performance through the provision of timely warnings to the user when it fails to meet certain margins of accuracy. The SoL service has been designed to be compliant to different standards in the aeronautical, maritime, and railway domains to maximize the benefit of the user community [5]. As of 2011, the SoL service is being re-profiled [46; 47].

### 4.2.3. Galileo Commercial Service (CS)

The Galileo Commercial Service allows for development of applications for professional or commercial use owing to improved performance and data as compared to the Open Service. It provides added value services on payment of a fee. It uses a combination of two encrypted signals for higher data throughput rate and higher accuracy authenticated data [47].

### 4.2.4. Galileo Public Regulated Service (PRS)

The Galileo Public Regulated Service provides position and timing to specific users that require a high continuity of service, with controlled access. It provides a continuous, robust, and encrypted signal that will be usable even in situations of crises, while the other services will be either deactivated or intentionally jammed [5]. Two PRS navigation signals with encrypted ranging codes and data will be available. This service is restricted to government-authorized users. It is targeted for security and strategic infrastructure (for example, energy, telecommunications and finance). The Galileo PRS is accessible through two Galileo signals, E1 and E6 [47].

### 4.2.5. Galileo Support to Search and Rescue Service (SAR)

The Galileo Support to Search and Rescue Service represents the contribution of Europe to the international COSPAS-SARSAT co-operative effort on humanitarian search and rescue activities. The international COSPAS-SARSAT programme provides accurate, timely, and reliable distress alert and location data to help search and rescue authorities assist persons in distress [48]. Through SAR service, Galileo satellites will be able to receive signals from emergency beacons carried on ships, planes or persons and transmits to national rescue centers. Thus, a rescue center can know the precise location of an accident. At least, one Galileo satellite will be in view of any point on Earth, so near real-time distress alert is possible [47].

## 4.3. Galileo Modulations

In this section, different signal modulations that will be used in Galileo systems are explained.

### 4.3.1. Binary Offset Carrier (BOC)

The concept of BOC modulation was first published by Betz as an effort for GPS modernization [29]. BOC modulation is a square sub-carrier modulation, where a signal is multiplied by a rectangular sub-carrier frequency $f_{sc}$. This frequency splits the signal spectrum into two parts. A BOC modulation is defined as BOC(m,n), where $m = {f_{sc}}/{f_0}$ and $n = {f_c}/{f_0}$, where $f_c$ is chip rate and $f_0 = 1.023\ MHz$ is the GPS reference frequency. From the equivalent baseband signal point of view, the BOC modulation can be defined via a single parameter, denoted as the BOC modulation order [29]:

$$N_{BOC} \triangleq 2\frac{m}{n} = 2\frac{f_{sc}}{f_c} \tag{4.1}$$

Where $m$ and $n$ are two positive indices, should be chosen in such a way that $N_{BOC}$ remains an integer.

BOC modulation has two main variants: sine-BOC (SinBOC) and cosine-BOC (CosBOC). Any SinBOC or CosBOC-modulated signal $x(t)$ can be seen as the convolution between Sin/CosBOC waveform and a modulating waveform $d(t)$, as follows [37]:

$$\begin{aligned} x(t) &= \sum_{n=-\infty}^{+\infty} b_n \sum_{k=1}^{S_F} C_{k,n} S_{Sin/CosBOC}\left(t - nT_{sym} - kT_c\right) \\ &= S_{Sin/CosBOC}(t) \otimes \sum_{n=-\infty}^{+\infty} \sum_{k=1}^{S_F} b_n C_{k,n} \delta(t - nT_{sym} - kT_c) \\ &\triangleq S_{Sin/CosBOC}(t) \otimes d(t) \end{aligned} \tag{4.2}$$

Where $\otimes$ is the convolution operator, $d(t)$ is the spreading sequence, $b_n$ is the *n*th complex data symbol (in case of pilot channel, it is equals to 1), $T_{sym}$ is the symbol period, $C_{k,n}$ is the *k*th chip corresponding to the *n*th symbol, $T_C = 1/f_c$ is the chip period, $S_F$ is the spreading factor ($S_F = T_{sym}/T_c$), and $\delta(t)$ is the Dirac pulse.

According to its original definition in Reference [38], $S_{SinBOC}$, $S_{CosBOC}$ and their equivalence are shown in Eq. (4.3) and Eq. (4.4) [37].

$$\begin{cases} S_{SinBOC}(t) = sign\left(sin\left(\frac{N_{BOC}\pi t}{T_c}\right)\right), 0 \le t \le T_c \\ S_{CosBOC}(t) = sign\left(cos\left(\frac{N_{BOC}\pi t}{T_c}\right)\right), 0 \le t \le T_c \end{cases} \tag{4.3}$$

$$\begin{cases} S_{SinBOC}(t) = P_{T_{B_1}}(t) \otimes \sum_{i=0}^{N_{BOC}-1} (-1)^i \delta\left(t - iT_{B_1}\right), \quad 0 \le t \le T_c \\ S_{CosBOC}(t) = P_{T_{B_1}}(t) \otimes \sum_{i=0}^{N_{BOC}-1} \sum_{k=0}^{1} (-1)^{i+k} \delta\left(t - iT_{B_1} - \frac{kT_{B_1}}{2}\right), 0 \le t \le T_c \end{cases} \tag{4.4}$$

Where $sign(\cdot)$ is the signum operator, $N_{BOC}$ is the BOC modulation order defined in Eq. (4.1), $P_{T_{B_1}}(\cdot)$ is the rectangular pulses of amplitude 1 and support $T_{B_1} = T_c/N_{BOC}$.

### 4.3.2. Multiplexed BOC (MBOC)

MBOC is optimized spreading modulation technique designed for the modulation of GPS L1C signal and Galileo E1 OS signal. This MBOC modulation design places a small amount of additional power at higher frequencies in order to improve the signal tracking performance [39]. The MBOC signal is obtained by multiplexing a standard BOC(1,1) with a BOC(6,1). The effect of the BOC(6,1) sub-carrier is an increased amount of power on higher frequencies, yielding to signals with narrower correlation functions and enables better performance at the receiver level. The power spectral density (PSD) of the entire MBOC signal is denoted as MBOC(6,1,1/11), where the term (6,1) refers to the BOC(6,1) and the ratio (1/11) represents the power split between the BOC(1,1) and BOC(6,1) spectrum components. The normalized PSD is defined as [29; 32]:

$$G_{MBOC(6,1,1/11)}(f) = \frac{10}{11} G_{SinBOC(1,1)}(f) + \frac{1}{11} G_{SinBOC(6,1)}(f) \tag{4.5}$$

Where $G_{SinBOC(m,n)}$ is the unit-power PSD of a sine-phased BOC modulation and 1/11 denotes the percentage of power of SinBOC(6,1) with respect to the total MBOC signal power. The MBOC PSD in Eq. (4.5) is the total PSD of pilot and data signals together. There are two main implementations to achieve MBOC PSD: Composite BOC

(CBOC) and Time-Multiplexed BOC (TMBOC), which are currently selected for Galileo E1 and modernized GPS L1 signals, respectively.

### 4.3.3. Composite BOC (CBOC)

Composite BOC modulation is currently the modulation assigned for Galileo Open Service in E1 band, according to Galileo Signal in Space-Interface Control Document (SIS-ICD) [42]. A CBOC implementation is based on the four level spreading symbols formed by the sum of the weighted SinBOC(1,1) and SinBOC(6,1) symbols as shown in Eq. (4.6) [29].

$$s_{CBOC}(t) = w_1 s_{SinBOC(1,1),held}(t) \pm w_2 s_{SinBOC(6,1)}(t) \tag{4.6}$$

In the Eq. (4.6), SinBOC(1,1) part is passed through a hold block in order to match the rate of SinBOC(6,1) part. The factors $w_1$ and $w_2$ are amplitude weighting factors which need to be chosen in such a way that PSD is as in Eq. (4.5) and ${w_1}^2 + {w_2}^2 = 1$. The CBOC modulation used in Galileo E1 consists of 10/11 of power from SinBOC(1,1) and 1/11 of power from SinBOC(6,1) [43].

In the above Eq. (4.6), when the two right-hand terms are added, CBOC('+') is formed, and when they are subtracted, CBOC('-') is formed. Currently, CBOC('+') is used for E1B data channel and CBOC('-') for E1C pilot channel in Galileo E1 signal [29; 32]. Figure 4.3 provides a generic view of the E1 CBOC signal generation.

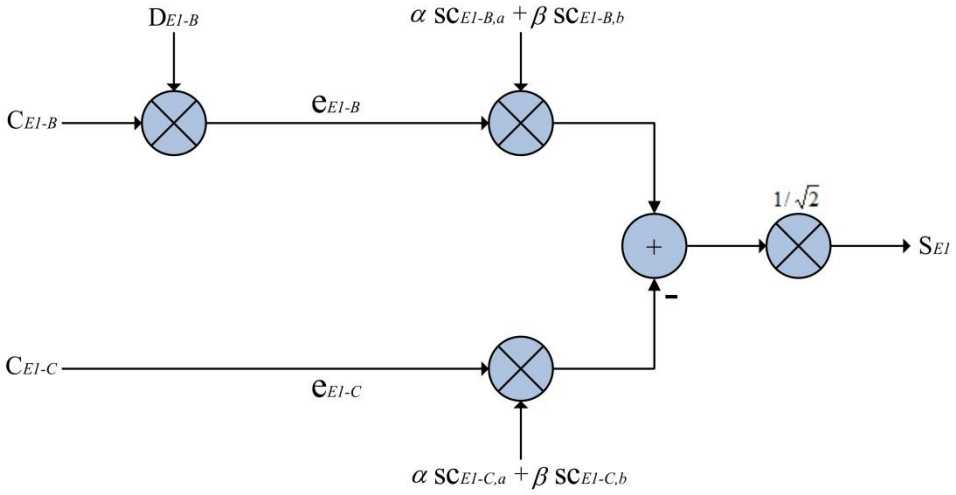


***Figure 4.3.*** *Modulation Scheme for the E1 CBOC Signal*

The E1 CBOC signal components are generated as follows:

- $e_{E1-B}$ from the I/NAV navigation data stream $D_{E1-B}$ and the ranging code $C_{E1-B}$, then modulated with the sub-carriers $sc_{E1-B,a}$ and $sc_{E1-B,b}$

- $e_{E1-C}$ (pilot component) from the ranging code $C_{E1-C}$ including its secondary code, then modulated with the sub-carriers $sc_{E1-C,a}$ and $sc_{E1-C,b}$

I/NAV is the integrity navigation message type provided by E1-B signal, supporting Safety of Life service and providing extended system integrity information [4]. The parameters $\alpha$ and $\beta$ are chosen such as that the combined power of the $sc_{E1-B,b}$ and $sc_{E1-C,b}$ subcarrier components equals 1/11 of the total power of $e_{E1-B}$ and $e_{E1-C}$. This result [4], $\alpha = \sqrt{\frac{10}{11}}, and\ \beta = \sqrt{\frac{1}{11}}$.

### 4.3.4. Time Multiplexed BOC (TMBOC)

In TMBOC modulation, the whole signal is divided into blocks of *N* code chips. *M* of *N* code chips (*M*<*N*) are SinBOC(1,1) modulated, while *N* – *M* code chips are SinBOC(6,1) modulated. The choice of *N* and *M* parameters depends on the power percentage of pilot channels with respect to the data channel [29].

### 4.3.5. Alternative BOC (AltBOC)

The AltBOC modulation is employed by the Galileo E5 signal and is the modulation employed in this thesis work. AltBOC modulation is a modified version of a binary offset carrier with a code rate of 10.23 MHz and a sub-carrier frequency of 15.345 MHz. AltBOC(15,10) is a wideband signal that is transmitted at 1191.795 MHz. The subcarrier waveforms are chosen so as to obtain a constant envelope at the transmitter. The result of this constant envelope AltBOC modulation is a split spectrum around the center frequency (E5a and E5b). Each sideband comprises two PRN codes modulated onto the orthogonal components. The in-phase components E5aI and E5bI carry the navigation messages. The quadrature components E5aQ and E5bQ are data free pilot signals [29].

The expression of the constant envelope AltBOC modulation PSD can be presented as [29],

$$G_{AltBOC(m,n)} = \frac{4}{\pi^2 f^2 T_c} \frac{cos^2(\pi f T_c)}{cos^2(\pi f \frac{T_c}{N})} \begin{bmatrix} cos^2\left(\pi f \frac{T_s}{2}\right) - \cos(\pi f \frac{T_s}{2}) \\ -2\cos\left(\pi f \frac{T_s}{2}\right)\cos\left(\pi f \frac{T_s}{4}\right) + 2 \end{bmatrix} \quad (4.7)$$

where $m$ defines the sub-carrier rate, $n$ defines the spreading code rate, and $N = N_{BOC}$, is the BOC modulation order defined in Equation 4.1.

Figure 4.4 provides a generic view of the E5 signal AltBOC modulation generation [4]. The E5 signal components are generated according to the following:

- $e_{E5a-I}$ from the F/NAV navigation data stream $D_{E5a-I}$ modulated with the unencrypted ranging code $C_{E5a-I}$

- $e_{E5a-Q}$ (pilot component) from the unencrypted ranging code $C_{E5a-Q}$
- $e_{E5b-I}$ from the I/NAV navigation data stream $D_{E5b-I}$ modulated with the unencrypted ranging code $C_{E5b-I}$
- $e_{E5b-Q}$ (pilot component) from the unencrypted ranging code $C_{E5b-Q}$

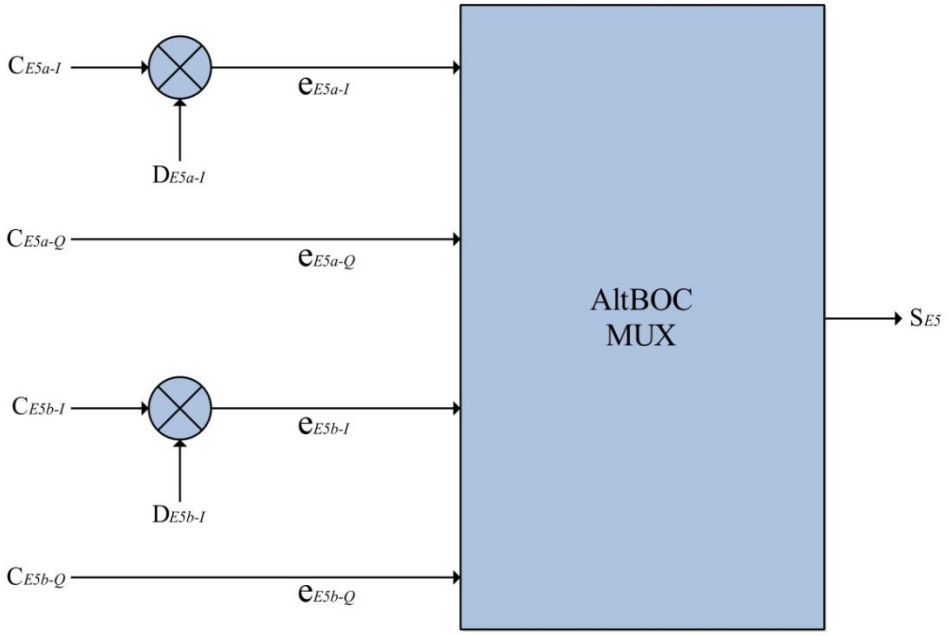


***Figure 4.4.*** *Modulation Scheme for the E5 signal (reproduced from [4]).*

F/NAV is the freely accessible navigation message provided by the E5a signal for Open Service, while I/NAV is the integrity navigation message type provided by E5b signal, supporting Safety of Life Service[4].

### 4.3.6. Binary Phase Shift Keying (BPSK)

The BPSK modulation is a very important and useful modulation in satellite navigation, which was in fact the first one to be used for satellite navigation [29]. A BPSK-modulated signal can be expressed as the convolution between a code part $d(t)$ (including navigation data) and a modulation pulse as [29]:

$$s(t) = p_{T_c}(t) \otimes \sum_{n=-\infty}^{+\infty} b_n \sum_{k=1}^{S_F} c_{k,n}\delta\left(t - nT_{sym} - kT_C\right),\ b_n = \begin{cases} +1\ for\ symbol\ "1" \\ -1\ for\ symbol\ "0" \end{cases} \quad (4.8)$$

$$= s_{BPSK} \otimes d(t)$$

Where $\otimes$ is the convolution operator, $T_c$ is the chip period, $b_n$ is the $n^{th}$ complex data symbol, $d(t)$ is the data sequence after spreading, $\delta(t)$ is the Dirac Pulse function, $T_{sym}$ is the code symbol period, $c_{k,n}$ is the $k^{th}$ chip corresponding to the $n^{th}$ symbol, $S_F$

is the spreading factor ($S_F = T_{sym}/T_C$), $p_{T_c}(t)$ is a rectangular pulse of unit amplitude and width $T_c$.

When a navigation data bit transition occurs, the phase of the resulting signal is phase-shifted by 180º [3]. In literature, BPSK(n) form is commonly used, which describes a signal with BPSK modulation and the spreading code rate n*1.023 MHz. The Galileo E5a and Galileo E5b signals employ BPSK(10) modulation. It is because, the AltBOC(15,10) modulation is very similar to two BPSK(10) signals shifted by 15 MHz to the left and right of the carrier frequency [40; 45]. The normalized PSD of a BPSK signal under ideal codes assumption can be defined as [44],

$$G_{BPSK}(f) = f_c \left( \frac{\sin(\pi f / f_c)}{\pi f} \right)^2 \tag{4.9}$$

## 4.4. Galileo Signals Structure

The description of the Galileo signal structure is based on the ICD open signals [4]. A number of different ranging codes and navigation messages had to be specified to meet the various application requirements of the Galileo services. Three types of ranging codes are distinguished: the open-access ranging code (which is not encrypted and publicly known), the ranging codes encrypted with commercial encryption, and the ranging codes encrypted with the governmental encryption [5]. The carrier frequencies of Galileo frequency bands are listed in Table 4.1. All satellites use the same carrier frequencies for signal transmission. The signals are differentiated by their spread spectrum using the principles of Code Division Multiple Access (CDMA).

A general power spectral density envelope of the Galileo signals is presented in [5]. All the Galileo signals, except the PRS components E6A and E1A, come in pairs. That is, the signals are transmitted in the pair of data channel and pilot channel in orthogonal planes. The data channel contains the ranging code sequence along with navigation messages whereas the pilot channels are the dataless signals that consist of the ranging code sequence only. The pilot channel allows for long coherent integration time, thereby sensing even weak signals [5].

The Galileo ranging codes consists of primary and secondary codes. Long spreading primary codes are generated by a tiered code construction, whereas a secondary code sequence is used to modify successive repetitions of a primary code periods. Figure 4.5 presents a method of generating tiered code.

In Figure 4.5, a primary code has a length $N_p$ and chip rate $f_c$, and a secondary code is of length $N_s$ and chip rate $f_{cs} = f_c/N$. The duration of N chips is also called a primary code epoch. In logical representation, the secondary code chips are sequentially exclusive-ored with the primary code, always one chip of the secondary code per period of the primary code [4]. The code length of tiered code sequence $N$ is [5],

$$N = N_p N_S$$

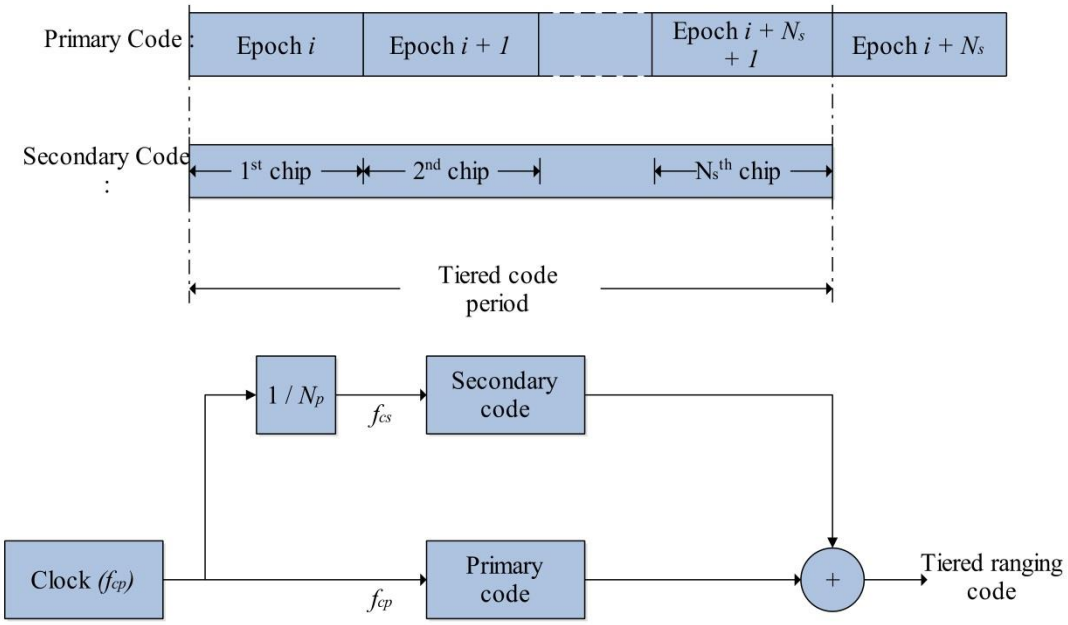


***Figure 4.5.*** *Tiered Codes Generation (reproduced from [4]).*

### 4.4.1. Primary Codes Generation

The primary spreading code sequences are either generated using a linear feedback shift register (LFSR) or they are optimized, constructed codes stored in satellite memory [4]. In case of memory codes, the Galileo primary codes are provided in the Galileo ICD document [4]. In case of LFSR, the code sequences are generated by an exclusive OR of two maximal lengths LFSR sequences that are short cycled after the code length as specified in Table 4.2.

***Table 4.2.*** *Galileo ranging code length*

| ***Signal Component*** | ***Tiered Code Period (ms)*** | ***Code Length (chips)*** | |
|---|---|---|---|
| | | ***Primary*** | ***Secondary*** |
| E5a-I | 20 | 10230 | 20 |
| E5a-Q | 100 | 10230 | 100 |
| E5b-I | 4 | 10230 | 4 |
| E5b-Q | 100 | 10230 | 100 |
| E1-B | 4 | 4092 | N/A |
| E1-C | 100 | 4092 | 25 |

For LFSR, the ICD specifies unique octal numbers, which indicate the registers to be used. Each shift register of length $R$ is fed back with a particular set of feedback taps. The content of the two shift registers is reset after $N$ cycles. The detailed description of

primary code generation for Galileo signals with LFSR, as well as the the families of primary codes and their assignment to satellites is provided in [4].

### 4.4.2. Secondary Codes

The secondary codes are fixed sequences as defined in hexadecimal notation in the Galileo ICD document provided [4]. Table 4.3 shows the secondary code assignment to the primary codes. The secondary code length can be 4, 20, 25, and 100 bits. For the 4, 20, and 25 bit secondary codes, the same code is used for all associated primary codes. For the 100 bits codes, an independent secondary code is assigned for each primary code. The secondary code $CS20_1$ is assigned to E5a-I for all satellites, $CS4_1$ is assigned to E5b-I for all satellites, and $CS25_1$ is assigned to E1-C for all satellites. But independent CS100 code is assigned for E5a-Q, E5b-Q, and E6-C. The families of secondary codes as well as their assignment to satellites are given in [4].

***Table 4.3.*** *Secondary Code Assignment [4].*

| ***Component*** | ***Secondary Code Assignment*** |
|---|---|
| E5a-I | $CS20_1$ |
| E5a-Q | $CS100_{1\text{-}50}$ |
| E5b-I | $CS4_1$ |
| E5b-Q | $CS100_{51\text{-}100}$ |
| E6-B | N/A |
| E6-C | $CS100_{1\text{-}50}$ |
| E1-B | N/A |
| E1-C | $CS25_1$ |

## 4.5. Galileo Signals

### 4.5.1. Galileo E1 Signal

Three navigation signal components are modulated onto the carrier frequency E1. The OS signals E1B and E1C are unencrypted and accessible to all users [5]. E1B is the data channel, and E1C is the pilot channel. The signal components E1B and E1C support the OS, CS, and SoL services. The E1A signal component is encrypted and only accessible to authorized PRS users. The ranging sequences E1B and E1C employs CBOC(6,1,1/11) modulation and E1A employs cosBOC(15,2.5) modulation [49]. The Galileo ICD for open signals has defined 50 unique pseudorandom memory code sequences for the primary codes of E1B and E1C. The code sequence for E1A is not published. Table 4.4 summarizes the technical characteristics of all the Galileo signals in E1 band. N/A stands for unknown values (due to not available public information).

***Table 4.4.*** *The technical characteristics of the Galileo E1 signals [49].*

| **GNSS System** | Galileo | Galileo | Galileo |
|---|---|---|---|
| **Service Name** | E1OS | | PRS |
| **Centre Frequency** | 1575.42 MHz | | |
| **Frequency Band** | E1 | | |
| **Access Technique** | CDMA | | |
| **Spreading Modulation** | CBOC(6,1,1/11) | | cosBOC(15,2.5) |
| **Sub-carrier frequency** | 1.023 MHz and 6.128 (Two sub-carriers) | | 15.345 MHz |
| **Code Frequency** | 1.023 MHz | | 2.5575 MHz |
| **Signal Component** | Data | Pilot | Data |
| **Primary PRN Code Length** | 4092 | | N/A |
| **Code Family** | Random Codes | | N/A |
| **Secondary PRN Code length** | - | 25 | N/A |
| **Data rate** | 250 sps | - | N/A |

### 4.5.2. Galileo E6 Signal

Similar to E1, three ranging codes are modulated onto the carrier frequency E6. The first signal E6A is reserved for PRS, whereas the other two signals E6B and E6C are designated to the CS. The signals E6B is the data channel, and the signal E6C is the pilot channel. The signal component E6B is the result of the XOR-addition of the navigation data stream and the ranging code sequence. The signal components E6B and E6C employs BPSK(5) modulation with a chipping rate of 5.115 Mcps. On the other hand, the signal component E6A employs cosBOC(10,5) modulation scheme, with a code chipping rate of 5.115 Mcps and a sub-carrier frequency of 10.23 MHz [4][5]. Table 4.5 summarizes the technical characteristics of all the Galileo signals in E6 band.

***Table 4.5.*** *The technical characteristics of the Galileo E6 signals [49].*

| **GNSS System** | Galileo | Galileo | Galileo |
|---|---|---|---|
| **Service Name** | E6 CS data | E6 CS pilot | E6 PRS |
| **Centre Frequency** | 1278.75 MHz | | |
| **Frequency Band** | E6 | | |
| **Access Technique** | CDMA | | |
| **Spreading Modulation** | BPSK(5) | BPSK(5) | cosBOC(10,5) |
| **Sub-carrier frequency** | - | - | 15.345 MHz |
| **Code Frequency** | 5.115 MHz | | |

| **Signal Component** | Data | Pilot | Data |
|---|---|---|---|
| **Primary PRN Code Length** | 5115 | | N/A |
| **Code Family** | Memory Codes | | N/A |
| **Secondary PRN Code length** | - | 100 | N/A |
| **Data rate** | 1000 sps | - | N/A |

### 4.5.3. Galileo E5 Signal

The Galileo E5 signal carries four signal components: a pair of data and pilot channel in the frequency bands E5a and E5b each. All four OS signals have a chipping rate of 10.23 Mcps. The data channel in the E5a frequency band is denoted by E5a-I. It is modulated by an unencrypted ranging code which is a freely accessible navigation message. This data message has a low data rate of 50 bits per second (bps) that increases data demodulation robustness. The combination of high chipping rate of E5a with the low data rate and the pilot channel characteristics provides the reception in weak signal environments such as indoors. The data channel in the E5b frequency band is denoted by E5b-I. It carries unencrypted navigation data and integrity information which is used for SoL services [4; 5].

The signal components E5a and E5b are modulated onto the E5 carrier frequency using the AltBOC(15,10) modulation with a sub-carrier frequency of 15.315 MHz and a chipping rate of 10.23 Mcps. The Galileo E5 signal is a wideband signal with a bandwidth of 51.15 MHz. Such a wideband signal has low multipath errors and high code tracking accuracy. Table 4.6 summarizes the technical characteristics of all the Galileo signals in E5 band.

***Table 4.6.*** *The technical characteristics of the Galileo E5 signals [49].*

| **GNSS System** | Galileo | Galileo | Galileo | Galileo |
|---|---|---|---|---|
| **Service Name** | E5a data | E5a pilot | E5b data | E5b pilot |
| **Centre Frequency** | 1191.795 MHz | | | |
| **Frequency Band** | E5 | | | |
| **Access Technique** | CDMA | | | |
| **Spreading Modulation** | AltBOC(15,10) | | | |
| **Sub-carrier frequency** | 15.345 MHz | | | |
| **Code Frequency** | 10.23 MHz | | | |
| **Signal Component** | Data | Pilot | Data | Pilot |
| **Primary PRN Code Length** | 10230 | | | |
| **Code Family** | Combination and short-cycling of M-sequences | | | |
| **Secondary PRN Code length** | 20 | 100 | 4 | 100 |

| | | | |
|---|---|---|---|
| **Data rate** | 50 sps | - | 250 sps |

## 4.6. Galileo navigation message structure

The navigation message is carried only on the inphase component whereas the quadraphase component is data-free. Table 4.7 presents different message types transmitted by data channels. The F/NAV is the freely accessible navigation message provided by the E5a signal for Open Service. Similarly, I/NAV is the integrity navigation message type provided by E5b and E1-B signals, supporting SoL service and provident extended system integrity information, and C/NAV is the commercial navigation message type provided by the E6-B signal supporting Commercial Service.

***Table 4.7.*** *Message allocation and general data content [4].*

| Message Type | Services | Component |
|---|---|---|
| F/NAV | OS | E5a-I |
| I/NAV | OS/CS/SoL | E5b-I and E1-B |
| C/NAV | CS | E6-B |

The message includes parameters for position determination like ephemerides information, satellite clock reading, space vehicle identification, satellite status flag, and almanac information. The ephemerides for each Galileo satellite consist of 16 parameters. The total size of these parameters is 356 bits.

The navigation messages consist of a sequence of frames that in turn are composed of subframes. The subframe is composed of pages. The data is spread over this three-layer data structure depending on whether it has to be transmitted at fast, medium, or slow rates. Urgent data is transmitted by spreading it over few pages. Similarly, slow-rate data is spread over greater message structures (that is, frames) [4; 5].

Every message page contains synchronization word and the data field. The synchronization word is a binary pattern that is used to gain synchronization to the data fields. This synchronization word consists of *M* symbols that are modulated and encoded onto the satellite signal. For instance, the F/NAV message type uses a binary pattern of 12 symbols, whereas the I/NAV message uses 10 symbol preamble [4; 5].

Galileo applies a three-level error correction encoding strategy to decrease the bit error rate: a cyclic redundancy check (CRC), a half-rate convolutional forward error correction (FEC) encoding, and block interleaving. This strengthens the transmitted message while reducing the error rate [5].

The CRC bits allow detecting the corrupted data messages. The checksum does not take into account the synchronization pattern and the tail bits. The CRC parity block consists of 24 bits.

**F/NAV message**

The F/NAV message is provided by the E5a-I signal component. F/NAV message consists of frames with a length of 600 seconds length. A frame is subdivided into 12 subframes, each of length of 50 seconds. One subframe is furthermore divided into 5 pages with a length of 10 seconds each. The general page structure consists of the synchronization field and the data field. The F/NAV data field consists of a page type field, the navigation data field, the CRC bits, and the tail bits. The page type field is 6 bits and identifies the page content. The navigation data field is the length of 208 bits and transmits the almanac, the ephemerides data, and general satellite information. The latter two are transmitted in pages 1 to 4, while page 5 contains almanac information [4].

The satellites do not transmit the same subframe at the same instant of time. Different subframes contain different almanac information. Thus, when more than one satellite is tracked, demodulation of almanac information from several satellites becomes possible in a short period of time.

**I/NAV message**

The I/NAV message of E5b-I and E1-B provide a dual-frequency service, also called as frequency diversity. The channels transmit the same information in the same page layout, but with different page sequencing [5]. Two types of pages have been specified for the I/NAV message: the nominal and the alert page. Nominal pages have duration of 2 seconds transmitted sequentially in time in two parts of duration, 1 second for each signal component. The first part of a page is denoted as ‘even’ and the second is denoted as ‘odd’. Alert pages have duration of 1 second. They transmitted in two parts of 1 second each at the same epoch over the E5b-I and E1-B signal components. This transmission is repeated at the next epoch but switching the two parts between the components [4]. Similar to the nominal page, the alert page consists of an even/odd field, the type field, and a data field that is split in two pages [5].

The Galileo ICD document gives the detailed description about error correction encoding strategy. Similarly, the document provides detail information about page content, page layout, and frame layout for I/NAV message and F/NAV message [4]. Note that the C/NAV message format is not provided in the Galileo ICD document.

# 5. DEVELOPPED SIMULATOR

The simulator developed in this thesis had as a starting point the FGI-GSRx software GNSS receiver developped by Finnish Geodetic Institute (FGI), Department of Navigation and Positioning, Masala, Finland. This software receiver was originally designed and implemented at Danish GPS Centre at Aalborg University for acquisition and tracking of GPS L1 band signals only. Finnish Geodetic Institute developed and modified this software receiver in order to be able to acquire also the Galileo E1 signals and Beidou B1 signals.

In order to acquire the signal from Galileo E5a Band, some modifications were made in the code. This thesis presents the simulation and results based on the Matlab Simulink Galileo E5a band signal generated from TUT Matlab Simulator, and real time Galileo E5b band signal received from FGI. Thus, modifications need to be done accordingly while simulating with Simulink data and with real time data. The section below describes the modification done in some of the functions in the receiver code to acquire the Galileo E5a band signals.

## 5.1. Introduction to FGI-GSRx receiver

The software receiver version provided by FGI is FGI-GSRx, version 1 (v1). The FGI-GSRx software Galileo receiver is designed to run in the Graphical User Interface Design Environment (GUIDE) tool in Matlab. Figure 5.1 represents the higher level block diagram of the Galileo receiver from FGI-GSRx implementation. The acquisition block receives the IF samples. The acquisition block performs identification of satellite code and coarse estimation of time and delay and Doppler shifts. The acquired signals are passed to the tracking process. The tracking block gives fine estimation of time delay and Doppler shifts. Finally, the tracked signals are passed to the navigation data extraction block. The navigation data extraction block demodulates the data and estimates the PVT solution.

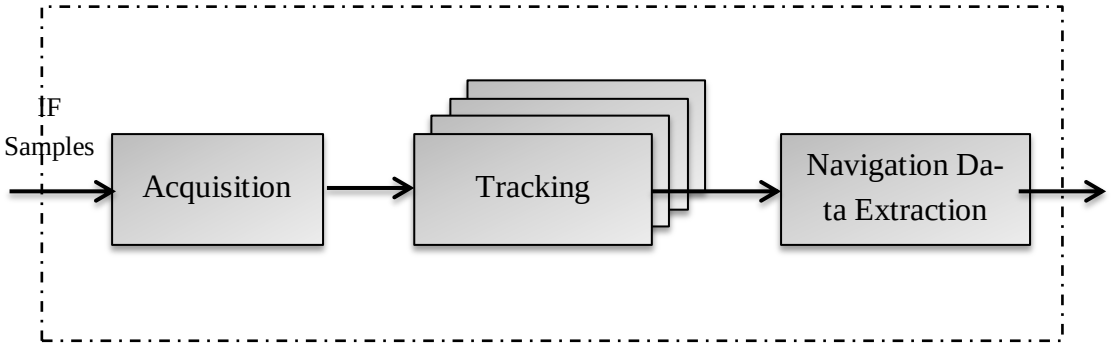


***Figure 5.1.*** *The functional block diagram of the software GNSS receiver*

Figure 5.2 presents the receiver settings in the GUIDE tool. As seen in the Figure 5.2, the path where the real time Galileo data file is stored can be loaded in GUI interface. Similarly, the parameters such as sampling frequency, number of milliseconds to process, IF frequency, etc. can be input by the user. Moreover, in the acquisition settings, the number of satellites can be chosen by the user. After all the parameters are set, when 'Processing' button is selected, the acquisition process is performed, and then the tracking process of the acquired satellites is performed.

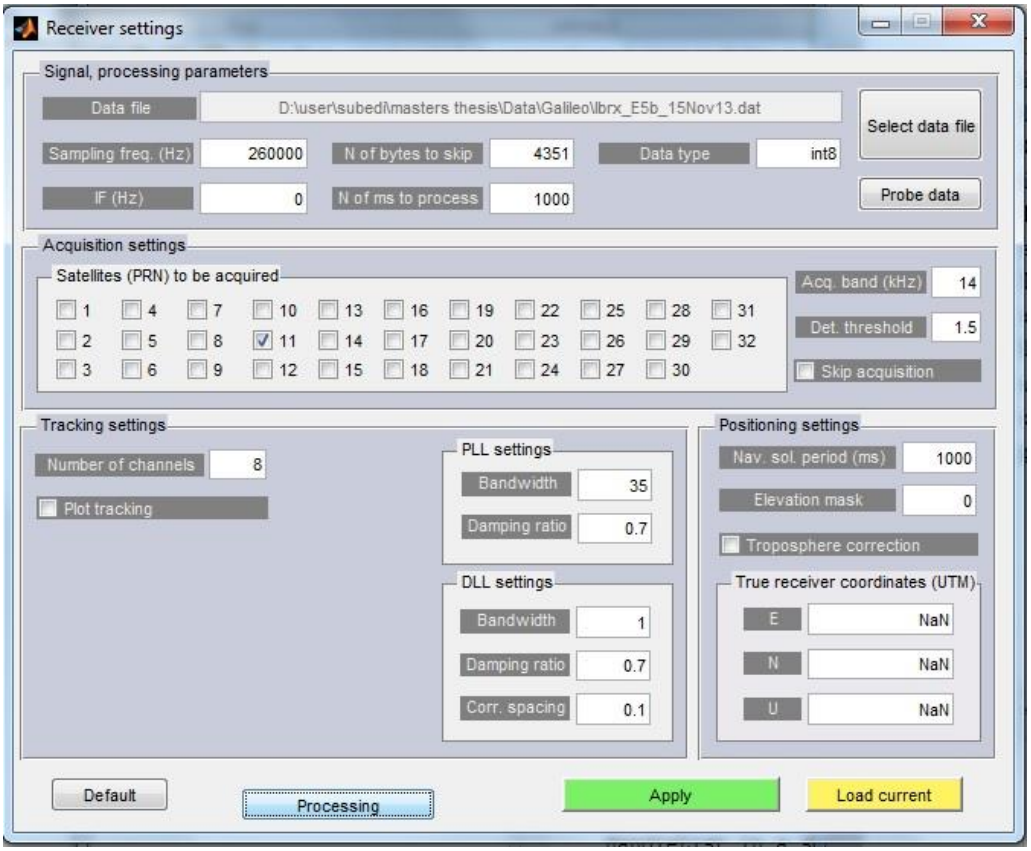


***Figure 5.2.*** *FGI-GSRx software receiver implementation in GUIDE tool of Matlab (reproduced from FGI-GSRx version 1 (v1))*

Figure 5.3 shows a block diagram showing the FGI-SRX GPS/Galileo implementation. The names of each block represent the function names. The function names are equal for both GPS and Galileo, except that for the Galileo implementation the "Galileo" term in italic is added. The program flow proceeds from the start point to the stop point unless no satellites are acquired. The child functions that are parallel in the diagram are called from the same parent function with a chronological order from left to right. Section below describes the program flow of the code as well as the modifications done in this thesis to acquire the Galileo E5 band signals.

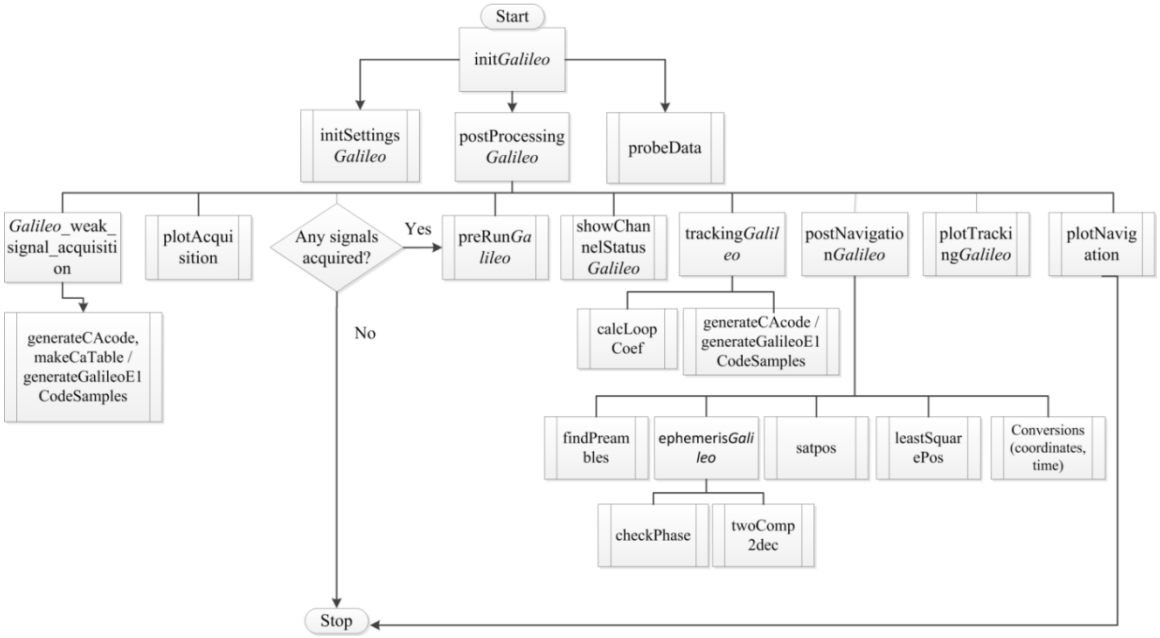


***Figure 5.3.*** *Block diagram of the FGI-SRX GPS/Galileo implementation [reproduced from FGI documentation for FGI-GSRx v1].*

## 5.2. The code structure

As mentioned in the above section, the program flow starts from start point in the Figure 5.3. The name of the block indicates the function name. The program flow starts from the function **initGalileo**.

From **initGalileo**, the program flows sequentially as:

- **initSettingsGalileo:**

This function defines the data file used and all parameters such as thresholds, loop parameters, channel to noise ratio, sampling frequency, intermediate frequency and so on.

- **probeData:**

This function plots raw data information that includes a time domain plot, a frequency domain plot and a histogram.

- **postProcessingGalileo:**

This function reads and processes the data. Following functions run sequentially in **postProcessingGalileo:**

- **Galileo_weak_signal_acquisition** (acquisition for all selected PRNs, it returns code phase and frequency)
- **plotAcquisition** (plot the results of acquisition)

(The program flow continues with below functions if at least one signal is acquired, otherwise the program stops processing.)

- **preRunGalileo** (initializes tracking channels)
- **showChannelStatus*Galileo*** (Prints the status of all channels in a table)
- **trackingGalileo** (code and carrier tracking for all channels, it returns in-phase prompt outputs and spreading code's starting positions, etc.)

- **postNavigationGalileo** (it provides navigation solution; pseudoranges and positions)
- **plotTrackingGalileo** (plot the results of tracking)
- **plotNavigation** (plot the results of navigation)

The focus of this thesis is only on acquisition and tracking part. Thus, the modification is done only in these parts to acquire and track the Galileo E5 band signals. All the other functionalities present in the FGI-GSRx are unchanged.

## 5.3. The settings structure

The settings structure stores all variables common to all receiver blocks in one structure. It is named as *settings*. This approach helps to centralize the software and makes the software flexible. For example, the sampling frequency-based parameters are used by many files, from acquisition function to pseudorange computation function. Once the parameters in the structure *settings* are updated, all files will use the changed values [3]. The most commonly used variables are:

- *IFfrequency* is the intermediate frequency of the GPS/Galileo signal, Hz.
- *codeFreqBasis* is the frequency of the Galileo code chip.
- *codeLength* is the number of chips in one Galileo code period.
- *samplingFrequency* is the frequency at which the GPS/Galileo signal is sampled, Hz.
- *msToProcess* is the total time of data to be processed.
- *processBlockSize* is the size of the block to be processed by the tracking function.
- *numberOfChannels* sets the number of channels of the software receiver.
- *nonCohIntNumber* sets the number of times non-coherent integration is to be performed.
- *cohIntNumber* sets the number of times coherent integration is to be performed.

Most of the parameters in the *settings* structure are same for both Galileo E1 band signals and Galileo E5 band signals. But, few parameters such as *IFfrequency, codeFreqBasis, codeLength,* etc., needs to be changed in order to receive the Galileo E5 band signals.

The *settings* structure is stored in the function **initsettingsGalileo**, and is executed by the script **initGalileo**. The function needs to be executed every time the variables are changed.

## 5.4. Acquisition function

The objective of acquisition function is to find signal parameters for all available satellites in a few-ms-long data record. The process of performing acquisition is same in both the Galileo E1 band signals and Galileo E5 band signals. That is, for both the cas-

es, FFT-based correlation is performed with the locally generated reference code for the user defined frequency bins. After that, the function looks for a correlation peak from all frequency bins. When a peak is detected, the function looks for the second-highest correlation peak in the same frequency bin of the highest peak. Thus, the ratio of the two peaks is used for the signal detection [3]. The fine carrier frequency is obtained if the value of the peak ratio is larger than a pre-defined threshold.

Although the acquisition is same for both Galileo E1 band signals and Galileo E5 band signals, the process of generating the reference code is different. Following function is used inside acquisition function to generate the reference code:
In case of Galileo E1 band signals**:**

- **generateGalileoE1CodeSamples** to generate the E1B and E1C codes.

In case of Galileo E5 band signals:

- **generateGalileoE5CodeSamples** to generate the E5aI and E5aQ (or E5bI and E5bQ) codes.

The method of generating Galileo E5 reference code is presented in Section 5.7.

## 5.5. Tracking Function

Similar to the acquisition function, the functionality of tracking function is same for both Galileo E1 band signals and Galileo E5 band signals. This function tracks the Galileo signals allocated to each channel. The function processes the block of the sample signals and return two structures: tracking results *trackResults* and an updated structure *channel*.

The structure *channel* contains current information on the carrier frequency, code phase, PRN number of the track satellite, temporary values for the loop filters, and local signal generators [3]. Similarly, the structure *trackResults* is the main output from tracking function. It stores results for all channels and information about signal properties (carrier frequency and code phase), and outputs from all six correlators and the loop discriminator.

The tracking function consists of following functions:

- **calcLoopCoef** calculates the loop coefficients.

In case of Galileo E1 band signals:

- **generateGalileoE1CodeSamples** to generate the E1B and E1C codes; early, prompt and late

In case of Galileo E5 band signals:

- **generateGalileoE5CodeSamples** to generate the E5aI and E5aQ (or E5bI and E5bQ) codes.

## 5.6. Function postNavigation

The input for **postNavigation** function is the output from tracking function. The function starts by finding bit transitions and preamble locations. Then the bit values are ob-

tained and the ephemerides are decoded. After that, the function calls the pseudorange measurement function and computes position coordinates for all tracked satellites. Pseudoranges are not computed for nontracking channels, for channels whose preambles are not detected, or for channels that have detected a parity error in the navigation data [3]. From the measured pseudoranges, the function **leastSquarePos** computes the position of the receiver. At the end of **postNavigation** function, the coordinates are transformed to UTM and geodetic coordinate systems. The results are stored in structure *navSolutions.*

## 5.7. Modification in the code to receive Galileo E5a band signals

Following sub-section discuss the modifications done in the FGI-GSRx receiver *v1* in order to receive and acquire the Galileo E5 band signals. As discussed earlier, this thesis is focused in simulation and analysis of both simulated as well as real time Galileo E5 band signals. The parameters in the settings structure needs to be changed accordingly. After the parameters are set, the signals can be acquired and tracked with the same functions for both the cases.

### 5.7.1. Settings structure

The values of all the parameters are not same when acquiring the simulated and real time Galileo E5 band signals. Given below are parameters that needs to be modified, and which are common when acquiring simulated Galileo E5 band signals and real time Galileo E5 band signals.

- *settings.codeFreqBasis* is set to $10.230 * 10^6$ [Hz], which is the chip rate of Galileo E5a band and E5b band signal.
- *settings.codeLength* is set to 10230, which is the length of the code of Galileo E5a band and E5b band signal.
- *settings.nonCohIntNumber* set to 20, which indicates the total non-coherent integration time is 20 ms.
- *settings.cohIntNumber* set to 1, which indicates the coherent integration time is set to 1 ms.

Similarly, the values of following parameters need to be changed when receiving real time and simulated Galileo E5 band signals.

For simulated Galileo E5 band signals:

- *settings.filename:* set to the location where the *mat* file is saved.
- *settings.IF* set to (20-15.345) MHz because the IF frequency of whole E5 band signal is set to 20 MHz in the TUT Simulator. Thus, Galileo E5a band signal has IF of (20-15.345) MHz.
- *settings.samplingFreq* set to 42 MHz.

- *settings.acqSatelliteList* set to [11] .

For real time Galileo E5 band signals:

- *settings.filename:* set to the location where the *dat* file is saved.
- *settings.IF* set to 0.
- *settings.samplingFreq* set to 26 MHz
- *settings.acqSatelliteList* set to [11 12 19 20] because the data are received from all four IOV satellites.

### 5.7.2. Acquisition function

In case of Galileo E5 band signals, the function **generateGalileoE5CodeSamples** generates the locally generated E5 code samples for a satellite from the array of satellites (1 to 30 satellites for Galileo). The array of satellites is defined in the *settings* structure, and the satellite number, whose PRN samples is need to be generated, is passed as a parameter in the function **generateGalileoE5CodeSamples**. The function **generateGalileoE5CodeSamples** first generates the PRN code of length 10230 using the method of LFSR as discussed in Section 4.4.1. This generated code is then sampled according to the sampling frequency defined in *settings* structure. The received Galileo E5a signal is then correlated with this generated E5 code and the results obtained (carrier frequency and code phase) is stored in the structure *acqResults.*

The function **generateGalileoE5CodeSamples** can generate the code samples for both Galileo E5a and Galileo E5b signals simultaneously for given satellite number. Thus the acquisition can be performed for both Galileo E5a and E5b band signals. The code sample of either Galileo E5a or Galileo E5b is passed to the acquisition function according to Galileo band predefined in the *settings* structure.

### 5.7.3. Tracking function

Tracking function is not implemented for real time Galileo E5 band signals. However for simulated Galileo E5 band signals, a method called ‘feed forward tracking’ is employed to track the acquired signals. In this method, the correlation between incoming signal and reference code is done, the same as in acquisition. But, the correlation is performed only in one carrier frequency which is obtained from acquisition. The tracking is performed in single channel as well as in two channel environments with certain level of $C/N_0$.

### 5.7.4. Navigation Function

As the thesis only focus on signal acquisition and tracking, thus the navigation part is not addressed for Galileo E5 band signals.

# 6. MEASUREMENT-BASED RESULTS

The main goal of this thesis, as stated in the introductory chapter, was to acquire the Galileo E5 band signals. For this, several modifications were done to the FGI-GSRx software GNSS receiver code provided by the FGI. The modifications were done as described in Chapter 5. The modified code can acquire either Galileo E5a band or Galileo E5b band signals, depending on the parameter defined in *settings* structure. At the time of writing this thesis, there were only four IOV satellites orbiting in the satellite constellation. For simplicity, those satellites are denoted by PRN numbers = 11, 12, 19, and 20, respectively. The testing was done via two approaches: 1. based on the E5 data generated from Simulink (with multipath and noise), and 2. based on the data collected by FGI from the real-time Galileo E5b band signals. The results obtained in both cases are discussed in the following sections. They show that the acquisition unit has been indeed implemented correctly.

## 6.1. Testing based on Simulink

Before testing the real time Galileo signal, the simulated Galileo signal was tested, which was created with the Simulink Galileo E1-E5 model of Tampere University of Technology, Tampere. As discussed in Section 3.5.8, the Galileo E5 Simulink model was designed at TUT under EU FP7 GRAMMAR project and it is able to generate Galileo E1 and E5 signals under a variety of multipath conditions and AWGN. Figure 6.1 shows the basic block diagram of the TUT Simulink model.

The E1 and E5 signals are generated in the transmitters according to the Galileo OS-SIS-ICD document [29]. In case of generating E5 signal, the whole E5 signal is generated by using AltBOC(15,10) modulation. The generated signal is then transmitted at Intermediate Frequency (IF) at the output of the transmitter. The generated signal is downconverted by the factor 3 and passed through the channel block. The generated signal is downsampled because sampling frequency can be lower since E5a signal has narrower bandwidth than E5 signal. The channel block generates the multipath signals and complex noise using a user-defined $C/N_0$, multipath delays, powers, and phases as input parameters [29]. The output from the channel is saved in a *mat* file in Matlab. This *mat* file is then loaded in the receiver code (created by the thesis' Author) and thus correlated with the locally generated Galileo E5a code.

In the Simulink model, the sampling frequency of Galileo E5 signal was set as $f_{s1} = 126\,MHz$, and the sampling frequency of the Galileo E5a signal was set as $f_s = 42\,MHz$.Similarly, the IF frequency of whole Galileo E5 band was set as, $f_{IF} =$

20 $MHz$. Now, the ***settings*** structure is set as defined in Section 5.7.1. in accordance with Simulink parameters.

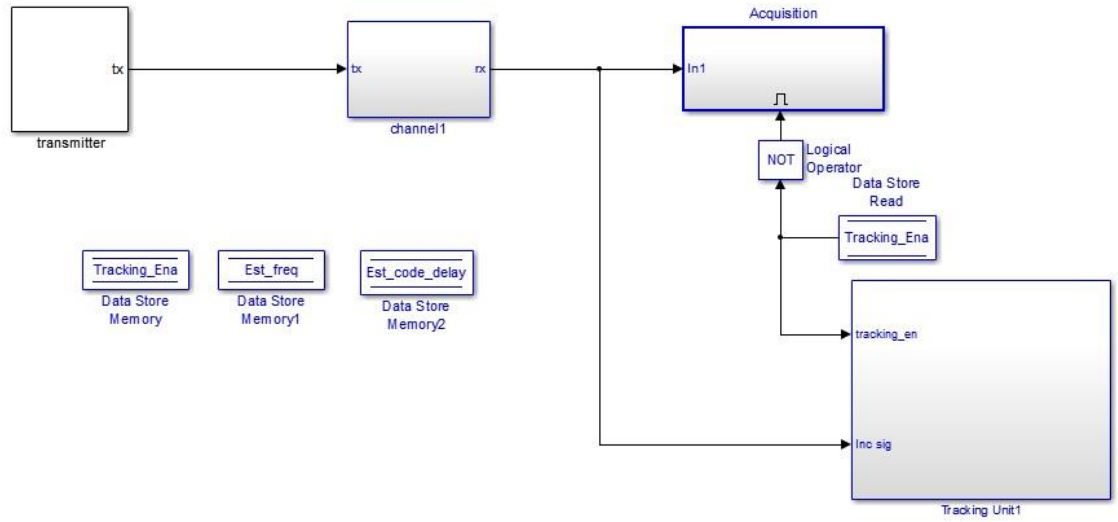


***Figure 6.1.*** *Generic TUT Galileo E1-E5 signal simulator structure.*

### 6.1.1. Acquisition results of Simulink-generated E5a signals

The Galileo E5a signal for PRN = 11 was generated in Simulink under various channel environments and each generated signal was loaded at the receiver code and correlated with the locally generated code. The acquisition results in different cases are shown in the figures below.

***a. Channel with multipath gain = [0], multipath delay = [0], and $C/N_0$= 60 dB***

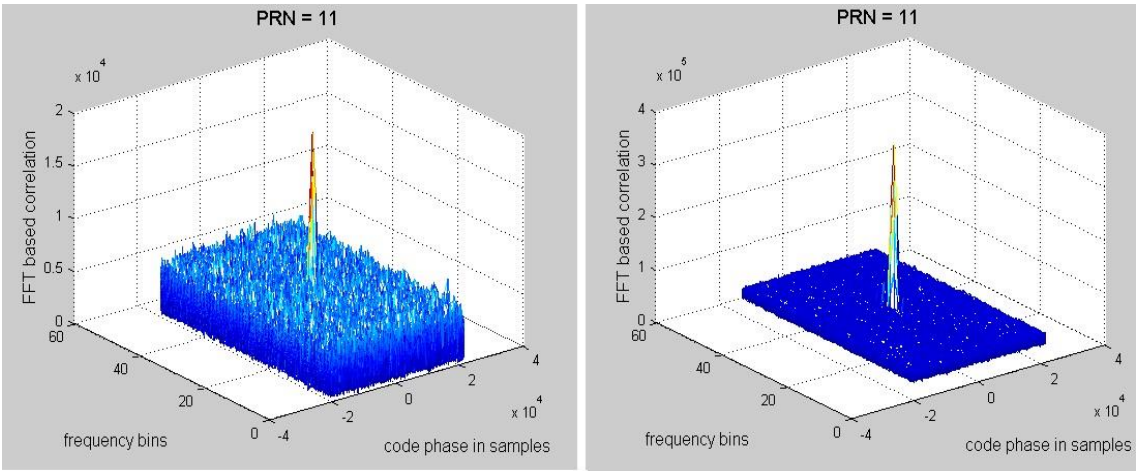


***Figure 6.2.*** *Time-frequency meshes in the E5a acquisition processing with $C/N_0$ = 60 dB; left with 2 ms non-coherent integration, right with 20 ms non-coherent integration.*

Figure 6.2 shows the acquisition plot when the Galileo E5a signal is transmitted through the channel with multipath gain = 0, multipath delay = 0, and $C/N_0$ = 60 dB. The figure in the left is obtained when the acquisition is performed for non-coherent

integration for 2 ms. The noise floor can be clearly seen in the plot. Similarly, the right plot in Figure 6.2. is obtained when the acquisition is performed for non-coherent integration for 20 ms. A more clear peak is obtained as the non-coherent integration time is increased.

### b. *Channel with multipath gain = [0 -3], multipath delay = [0 $3T_c$], and $C/N_0$= 50 dB*

Figure 6.3 shows the acquisition plot when the Galileo E5a signal is transmitted through a multipath channel with two paths, with multipath gains [0 -3], $C/N_0$ = 50dB, and multipath delays of [0 $3T_c$], where $T_c = 1/10.230 * 10^6$ seconds, is the chip rate of the code. As seen in the figure, when the $C/N_0$ is increased, then the noise floor gets high.

When the acquisition is performed with 2 ms non-coherent integration, then no peak is obtained. Similarly, a peak with less noise floor is obtained with 20 ms non-coherent integration (as seen in the right-hand plot of Figure 6.3). An even clear peak can be obtained with more non-coherent integration time.

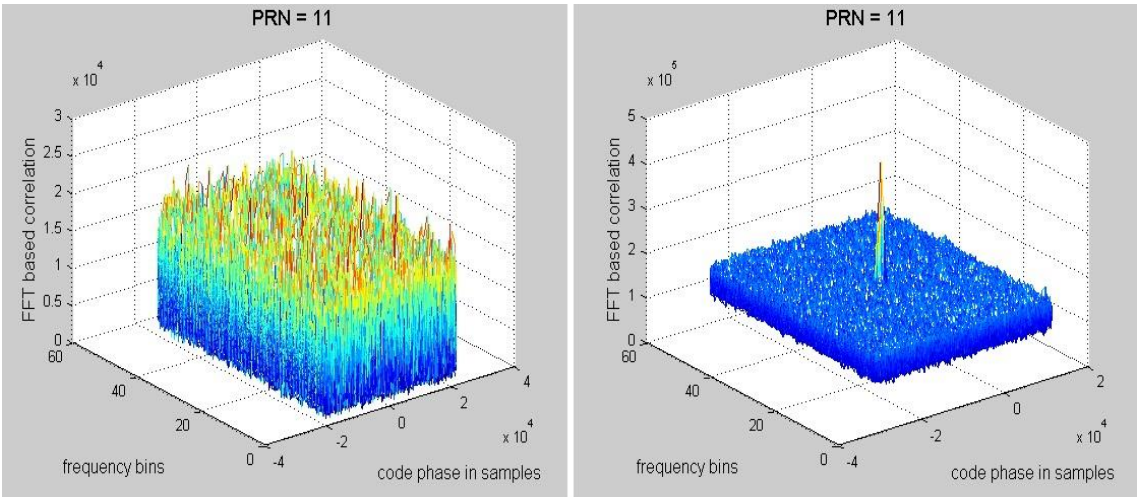


***Figure 6.3.*** *Time-frequency meshes in the E5a acquisition processing with multipath gain = [0 -3], multipath delay = [0 $3T_c$], and $C/N_0$ = 50 dB; left with 2 ms non-coherent integration, right with 20 ms non-coherent integration.*

### c. *Channel with multipath gain = [0 -3], multipath delay = [0 $3T_c$], and $C/N_0$ = 30 dB*

Figure 6.4 shows the acquisition plot when the Galileo E5a signal is transmitted through a multipath channel with two paths and multipath gains [0 -3], $C/N_0$ = 30dB, and multipath delay of [0 $3T_c$]. No peak is obtained, neither with 20 ms non-coherent integration nor with 500 ms non-coherent integration. This is due to rather low $C/N_0$ of 30dB.

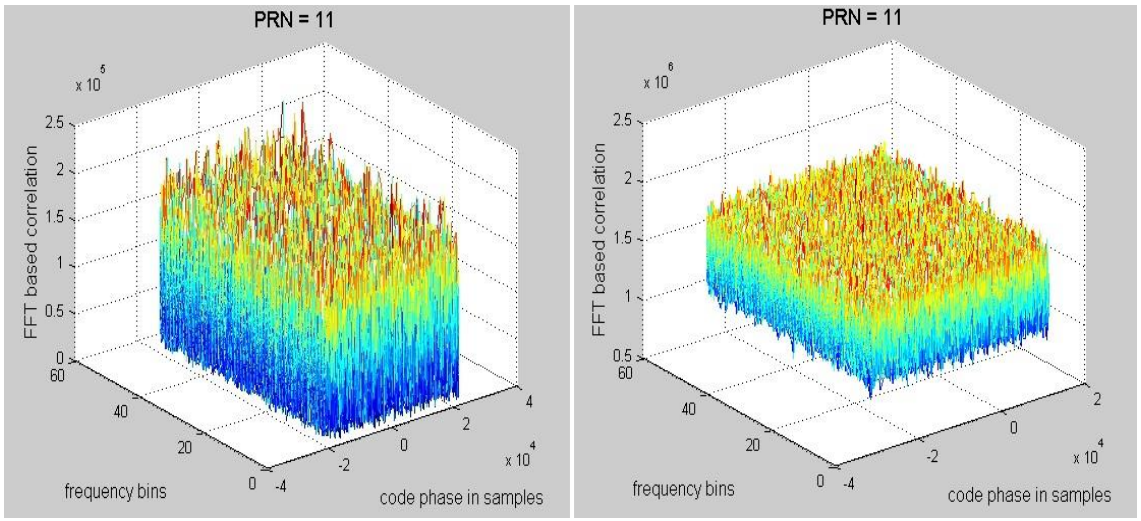


***Figure 6.4.*** *Time-frequency meshes in the E5a acquisition processing with multipath gain = [0 -3], multipath delay = [0* $3T_c$*], and* $C/N_0$ *= 30 dB; left with 20 ms non-coherent integration, right with 500 ms non-coherent integration.*

### 6.1.2. Tracking result of simulated signals

Tracking is done to find the exact code phase of the acquired signal. In this thesis, tracking was performed for two cases: a. channel with single path, and b. channel with multipath. The figures below are the results obtained in single channel and multipath channel environments.

***a. Channel with single path (multipath delay = [0], and*** $C/N_0$ ***= 60 dB)***

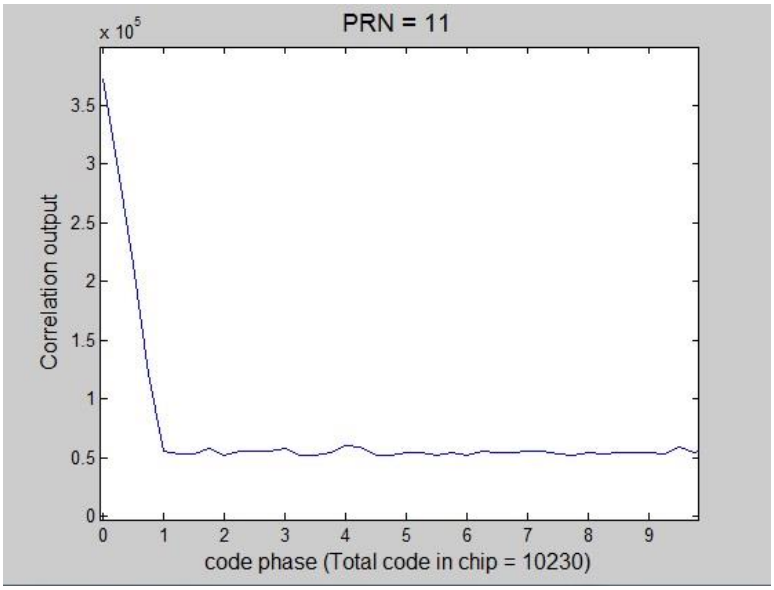


***Figure 6.5.*** *Code tracking of E5a signal in single path*

Figure 6.5 shows the code tracking of E5a signal in single path where multipath delay = [0] and $C/N_0$ = 60 dB**.** As the delay of the path is 0, the code phase difference between the incoming signal and local replica is zero. Thus, the peak is obtained at zero code phase.

### *b. Channel with multipath*

In this case, tracking was performed for two different multipath environments: 1. For multipath delay = [0 $3T_c$], and $C/N_0$= 60 dB; and 2. For multipath delay = [0 $4T_c$], and $C/N_0$= 60 dB.

Figure 6.6(i) is the plot when multipath delay = [0 $3T_c$]. As we have a two-path channel, two peaks are observed. The delay of first path is 0, thus the first peak is observed at 0 code phase. Similarly, as the delay of second path is $3T_c$, the second peak is observed after the three chips from the first peak.

Similarly, Figure 6.6(ii) is the plot when multipath delay = [0 $4T_c$]. The delay of second path is $4T_c$, thus the second peak is observed after 4 chips from first peak.

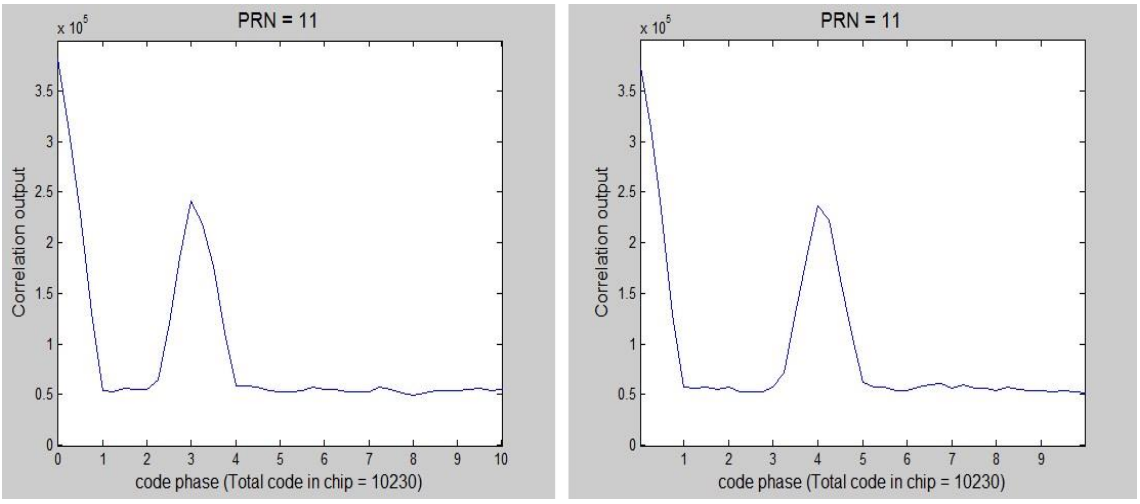


(i) (ii)

***Figure 6.6.****Code tracking versus code phase of E5a signal in multipath channel; (i) channel delay = [0 3Tc], (ii) channel delay = [0 4Tc]*

## 6.2. Measurement based on real time Galileo E5b band data

During the duration of thesis, we only had access to measured real-time Galileo E5b signals provided by FGI (for some reasons, the measurements of E5a signals were unsuccessful). The data provided is in the *dat* file format. As mentioned above, the receiver built by the Author can acquire either Galileo E5a band or Galileo E5b band signals depending on the parameter set in the *settings* structure. Similarly, parameters need to be set in the ***settings*** structure is defined in Section 5.7.1.

After the ***settings*** structure is initialized, the acquisition is performed and the time-frequency mesh of the result of the correlation between the real time data and the locally generated PRN codes are plotted. Figure 6.7 shows the time-frequency mesh for four different satellites (PRN 11, 12, 19, and 20). It can be seen from the figure that signals from four satellites are successfully acquired with a visible peak.

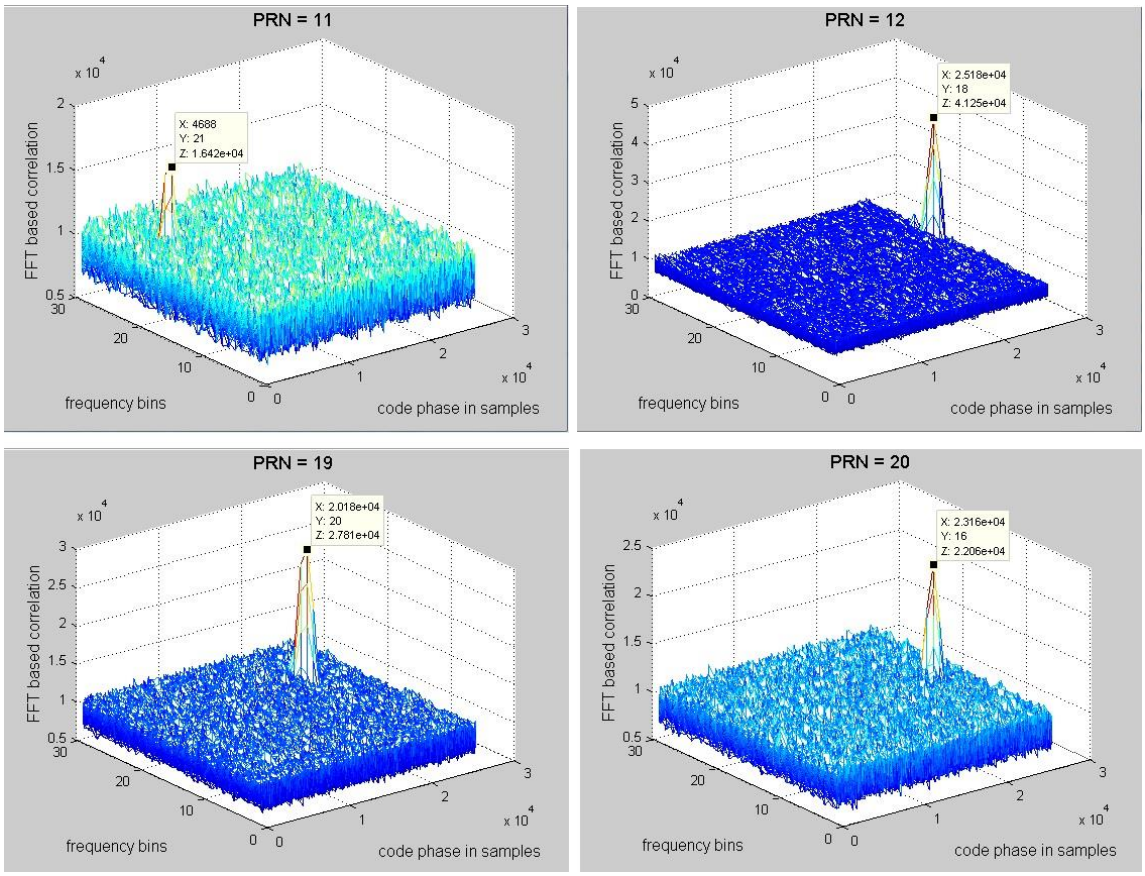


***Figure 6.7.*** *Acquisition of real time Galileo E5b signals for PRN 11, 12, 19, and 20*

A random check is performed by correlating the received signals with the locally generated codes for PRN 5, 6, 19, and 22. Figure 6.8 shows the acquisition mesh obtained when the received signals are correlated with the mentioned PRN codes and above settings structure. As expected, no correlation peaks are observed in Figure 6.8 for PRN 5, 6, and 22, because none of the tested PRNs in there were present on the sky.

After the correlation and finding out the highest peak, the second highest peak is analyzed. If the ratio of the highest peak to the second highest peak is greater than the certain predefined acquisition threshold, then the signals are considered to be acquired. Thus, the code phase and carrier frequency of acquired signals are saved in the *acqResults* structure and this structure is used for tracking process. Figure 6.9 presents an example showing which signal has been acquired in two cases: *(i)* when the received signals are correlated with the locally generated code for PRN 11, 12, 19, and 20. *(ii)* when the received signal are correlated with the locally generated code for PRN 5, 6, 19, and 22. The acquisition threshold value was set to 1.3.

From the Figure 6.9, the left plot shows that the satellite signals for PRN 11, 12, 19, and 20 are acquired (indicated by green color). Similarly, the right plot shows that only signal for PRN 19 is acquired and signals for PRN 5, 6, and 22 are not acquired (indicated by blue color). This is in tune with what satellite is present on the sky at the time of the measurements.

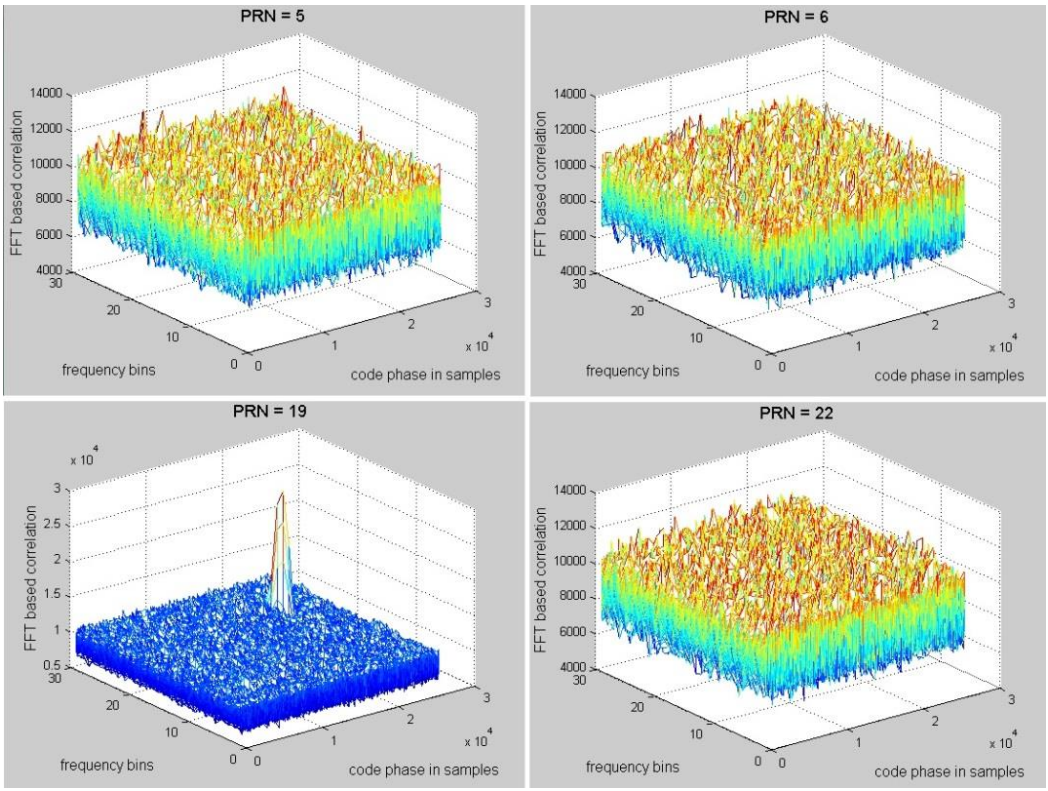


***Figure 6.8.*** *Acquisition of real time Galileo E5b signals for PRN 5,6,19, and 20*

The acquisition threshold should be chosen wisely so that all the received signals are acquired. Considering the left plot of Figure 6.9, the acquisition threshold is chosen as 1.3, and non-coherent integration time is set to 20. If the acquisition threshold were to be set to 2, then even though a peak would have been observed for PRN 11, the signal wouldn't have been acquired (because the ratio of highest peak to the second highest peak is less than 2).

Table 6.1 presents the number of satellites acquired when the threshold parameter is set to different values and the non-coherent integration time of 20 ms. From here, we can notice that the threshold selection plays an important role in the acquisition.

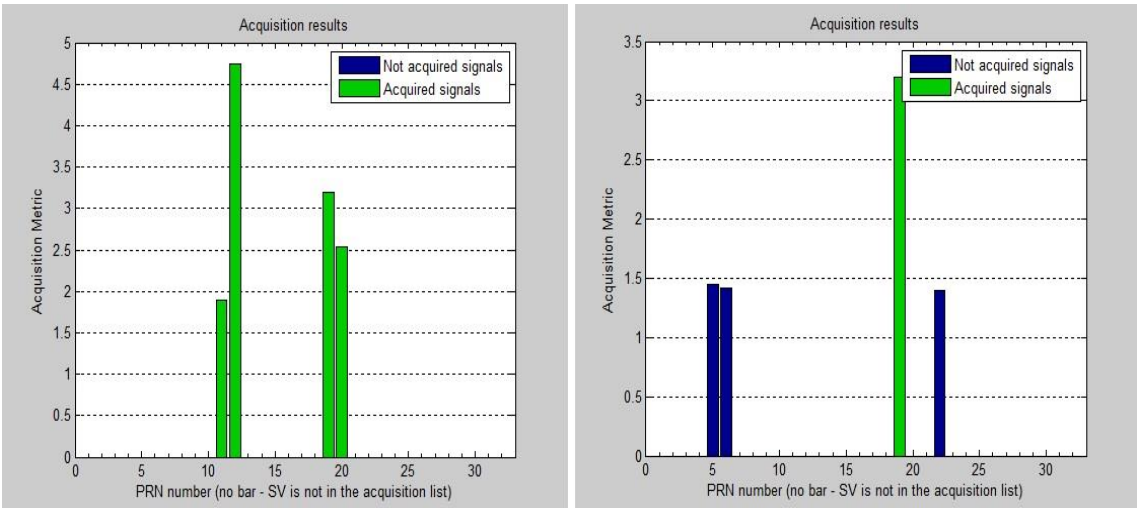


***Figure 6.9.*** *Acquisiton results when the received signals are correlated with locally generated code for PRN 11, 12, 19, and 20 (left); and PRN 5, 6, 19, and 22 (right)*

***Table 6.1.*** *No. of satellites acquired at different acquisition threshold values*

| Acquisition Threshold | No. of acquired satellites |
|---|---|
| 1.2 | 4 |
| 1.5 | 4 |
| 1.9 | 3 |
| 2.6 | 2 |
| 3.5 | 1 |

Regarding the tracking of the measured E5b signal, this was outside the scope of the thesis, due to the time constraints and due to the fact that the tracking model used for tracking the Simulink generated data was not working with the real-time signals, but needed more modifications.

# 7. CONCLUSIONS AND OPEN DIRECTIONS

This chapter summarizes the research results of the thesis. Similarly, the future continuation of the research is discussed.

## 7.1. Conclusions

The GNSS is currently playing a significant role in wireless communications. The GNSS is used to pinpoint the geographic location of a user's receiver anywhere in the world. Two GNSS systems are currently in full operational mode: the United States' Global Positioning System (GPS) and the Russian Federation's GLONASS. The European Galileo and the Chinese Beidou satellite system are estimated to be fully deployed by the years 2019-2020. At the time of writing this thesis, the Galileo system has launched four IOV satellites and the Beidou system has launched fourteen operational satellites in their respective constellations. The European Galileo system transmits signals in three frequency bands, - named as Galileo E1, E5, and E6 band. The Galileo E5 band is further divided in Galileo E5a and Galileo E5b bands. This thesis focused on signal acquisition of Galileo E5a band signals.

The objective of this thesis has been to extend the provided software to acquire the real-time Galileo E5a band signals as well as acquire and track the simulated Galileo E5a band signals. This simulator was implemented starting from the FGI-GSRx software Galileo receiver provided by the Finnish Geodetic Institute (FGI), Masala, Finland. The provided software could already successfully acquire and track the Galileo E1 band signals. The goal of this thesis was to extend the software receiver to acquire the real-time Galileo E5a band signals and this goal was achieved.

Before processing the real-time signals, the acquisition was first performed with the simulated Galileo signal generated with the Simulink E1-E5 model developed at Tampere University of Technology (TUT). This was done in order to verify whether the implemented simulator is working properly under controlled environment. The Simulink model generated signals was correlated with the locally generated PRN code in the various noise level and various channel delay profiles. Different kind of acquisition peaks were obtained depending on the channel delay profiles. A sharp triangular peak with certain level of noise floor was obtained with 20 ms of the non-coherent integration time. The noise floor was reduced when the non-coherent integration time was increased. After the acquisition, the tracking of the signals were performed. However, in tracking, the correlation is performed only in one frequency that was acquired from acquisition in single and two-path channel. A single peak was obtained for single-path channel, and two peaks were obtained for two-path channel. In the case of two-path

channel, the distance between two peaks depend on the value of delay applied in the channel.

After successfully acquiring the simulated Galileo E5a band signal, the acquisition was then performed with the real time Galileo E5b signals provided by FGI. The signals received were from all four IOV satellites currently on the sky with PRN 11, 12, 19, and 20. Four satellite signals were successfully acquired with certain level of noise floors as presented in Section 6.2. After the acquisition process, the obtained peak was compared to the certain pre-defined threshold. Thus the peaks which are greater than the pre-defined threshold were sent for the tracking process. Thus, the target of the thesis was successfully achieved both with the real time signals and the simulated signals.

## 7.2. Open directions

The developed FGI-GSRx simulator can successfully acquire the Galileo E1 and Galileo E5 band signals. The software needs to be further extended to acquire the Galileo E6 band signals. Similarly, the receiver can be extended to acquire and track the signals from the existing GLONASS navigation satellite system as well as from all the frequency bands of BeiDou satellite navigation system. Moreover, improvement in the receiver can be done by acquiring the signals from not only one type of GNSS system at a time, but from all the available GNSS systems continuously.

# REFERENCES


[1] C. J. Hegarty, E. Chatre, "Evolution of the Global Navigation Satellite System (GNSS)", *Proc. of the IEEE (Volum: 96, Issue 12)*, pp. 1902-1917, December 2008.

[2] E. Kaplan, C. Hegarty, *Understanding GPS: Principles and Applications*, 2nd ed. Norwood, MA: Artech House, 2006.

[3] K. Borre, D. M. Akos, N. Bertelsen, P. Rinder, S. H. Jensen, *A Software-Defined GPS and Galileo Receiver, A single-frequency approach,* Birkhäuser, 2007.

[4] *Galileo open service signal in space interface control document OS SIS ICS,* available via: http://ec.europa.eu/enterprise/policies/satnav/galileo/open-service/index_en.htm

[5] B. Hofmann-Wellenhof, H. Lichtenegger, E. Wasle, *GNSS-Global Navigation Satellite Systems,* New York: Springer-Verlag, 2008.

[6] *GLONASS global navigation satellite system interface control document*, Available via: http://www.sdcm.ru/smglo/staticpages?version=eng&site=extern &title= ref

[7] *BeiDou Navigation Satellite System In Space Interface Control Document, Open Service Signal (Version 2.0),* China Satellite Navigation Office, December 2013.

[8] *Comission Implementing Decision,* Official Journal of the European Union of 23 of February 2012, (2012/117/EU), Volume 55, Available via: http://eur-lex.europa.eu/legal-content/en/ALL/?uri=OJ:L:2012:052:TOC

[9] M. S. Grewal, A. P. Andrews, C. G. Bartone, *Global Positioning Systems, Inertial Navigation, and Integration,* 3rd Edition, March 2013.

[10] J. Spacek, P. Puricer, "Front-end Module for GNSS Software Receiver", *Proc. in Multimedia Signal Processing and Communications, 48th International Symposium ELMAR-2006,* pp. 211-214, June 2006, Zadar, Croatia.

[11] S. Gleason, D. Gebre-Egziabher (eds), *GNSS Applications and Methods,* Artech House, INC., 685 Canon Street, 2009, Norwood, MA.

[12] S. Jin (ed), *Global Navigation Satellite Systems: Signal, Theory and Applications,* pp. 107-126, *Published by InTech,* February, 2012. N. C. Shivaramaiah, A. G. Dempster, "Baseband Hardware Designs in Modernised GNSS Receivers", *book chapter 2 in S. Jin (Ed),* "Global Navigation Satellite Systems: Signal, Theory and Applications", ISBN978-953-307-843-4, InTech, February 2012.

[13] M. S. Sharawi, O. V. Korniyenko, "Software Defined Radios: A software GPS Receiver Example", *Proc. in Computer Systems and Applications, 2007.*

*AICCSA '07. IEEE/ACS International Conference,* pp. 562-565, May 2007, Amman, Jordan.

[14] Y. H. Chen, J. C. Juang, D. S. De Lorenzo, J. Seo, S. Lo, P. Enge, D. M. Akos, "Real-Time Dual-Frequency (L1/L5) GPS/WAS Software Receiver", *Proc. of the 24th International Technical Meeting of the Satellite Division of the Institute of Navigation,* pp. 767-774, September, 2011, Portland, OR, USA.

[15] SatNav News, Federal Aviation Administration, Volume 32, November 2007, via: www.faa.gov

[16] G. Heinrichs, M. Restle, C. Dreisher, T. Pany, "NavX®-NSR- A Novel Galileo/GPS Navigation Software Receiver", *20th International Technical Meeting of the Satellite Division of The Institute of Navigation, ION GNSS 2007,* pp. 1329-1334, September 2007, Fort Worth, Texas USA.

[17] C. Dionisio, D. Citterico, G. Pirazzi, N. De Quattro, L. Cucchi, R. Marracci, N. Valdambrini, I. Formaioni, "gLab a fully software tool to generate, process and analyze GNSS signals", *Satellite Navigation Technologies and European Workshop on GNSS Signals and Signal Processing (NAVITEC), 2010 5th ESA Workshop,* pp. 1-7, Dec. 2010, Noordwijk, Netherlands.

[18] X. Hu, E. S. Lohan, "GRANADA validation of optimized Multiple Gate Delay structures for Galileo SinBOC(1,1) signal tracking", *Published in Telecommunications, 2007. ITST '07. 7th International Conference on ITS,* pp 1-5, June 2007, Sophia Antipolis, France.

[19] T. Peres, J.S. Silva, P.F. Silva, J.M, Palomo, "GRANADA FActored Correlator Model blockset verification using an FPGA-based GNSS receiver", *Published in Satellite Navigation Technologies and European Workshop on GNSS Signals and Signal Processing (NAVITEC), 2010 5th ESA Workshop,* pp. 1-7, Dec. 2010, Noordwijk, Netherlands.

[20] A. Fernandez, P. D'Angelo, J. Diez, L. Marradi, V. Gabaglio, "Navigation Algorithm Optimisation for Combined Galileo/GPS Receivers with the GRANADA Environment and Navigation Simulator", *Proc. of the 18th International Technical Meeting of the Satellite Division of The Institute of Navigation (ION GNSS 2005),* pp. 1939-1944, Sept. 2005, Long Beach, CA.

[21] D. Skournetou, E. S. Lohan, "Ionospheric Delay Corrections in Multi-Frequency Receivers: Are Three Frequencies Better than Two?", *Published in Localization and GNSS (ICL-GNSS),* pp. 181-186, Jun 2011, Tampere, Finland.

[22] IFEN (2009). GALILEO & GNSS-2 – GNSS Software Simulation, *Institute of Geodesy and Navigation Official Site: http://www.ifen.unibw-muenchen.de/research/gnss_simulator.htm*, accessed: December 2013.

[23] GPSoft (2003). "MPGEN." Satellite Navigation TOOLBOX 3.0 User's Guide, Athens, Ohio, U.S.A., 146 p.

[24] A. Dolgansky, A. Szeto, and S. Bisnath, "Software Simulation of Multiple Global Navigation Satellite System Measurements", *Published in Science and Technology for Humanity (TIC-STH), 2009 IEEE Toronto International Conference,* pp. 322-327, Sept. 2009, Toronto, ON.

[25] Simulink open-source software for Galileo E1 and E5 signals, *http://www.cs.tut.fi/tlt/pos/Software.htm*, Tampere University of Technology, accessed December 2013.

[26] U. Engel, "A geolocation method using ToA and FoA measurements", *Published in Positioning, Navigation, and Communication, 2009. WPNC 2009. 6th Workshop,* pp. 77-82, March 2009, Hannover, Germany.

[27] Z. Deng, D Zou, J. Huang, X. Chen, Y.P. Yu, "The Assisted GNSS Boomed up Location Based Servces", *Published in Wireless Communications, Networking and Mobile Computing, 2009. WiCom '09, 5th International Conference,* pp. 1-4, Sept. 2009, Beijing, China.

[28] F. V. Diggelen, *A-GPS: Assisted GPS, GNSS, and SBAS,* Artech House, 2009.

[29] J. Zhang, "Advanced Signal Processing in Multi-mode Multi-frequency Receivers for Positioning Applications", Ph.D. Thesis, *Tampere University of Technology, Publication 1176,* Tampere 2013.

[30] P. G. Mattos, "Solutions to the cross-correlation and oscillator stability problems for indoor C/A code GPS", *Proc. of the 16th International Technical Meeting of the Satellite Division of The Institute of Navigation,* pp. 654-659, September 2003, Portland, OR, USA.

[31] M. Z. H. Bhuiyan, J. Zhang, E. S. Lohan, W. Wang, S. Sand, "Analysis of multipath mitigation techniques with land mobile satellite channel model", *Radioengineering,* vol. 21, no. 4, December 2012.

[32] J. Zhang, E. S. Lohan, "Multi-correlator structures for tracking Galileo signals with CBOC and SinBOC(1,1) reference receivers and limited front-end bandwidths", *Proc. of The 7th IEEE Workshop on Positioning, Navigation and Communication 2010 WPNC,* pp. 179-186, March 2010, Dresden, Germany.

[33] J. Zhang, D. Skournetou, W. Wang, S. Sand, E. S. Lohan, "Performance analysis of dual-frequency range estimation methods in the presence of ionospheric and multipath propagation effects", *Proc. of the International Conference on Localization and GNSS ICL-GNSS,* pp. 1-5, June 2012, Starnberg, Germany.

[34] H. Kuusniemi, M. Z. H. Bhuiyan, "Signal Barred", *Geospatial World, The Geospatial Industry Magazine,* pp. 31-33, November 2012.

[35] T. J. Grenchik, B. T. Fang, "Time Determination for Spacecraft Users of the Navstar Global Positioning System (GPS)", *31st Annual Symposium on Frequency Control,* 1977.

[36] Council Resolution of 19 July 1999 on the involvement of Europe in a new generation of satellite navigation services -Galileo- Definition phase (1999/C 221/01).

[37] E. S. Lohan, A. Lakhzouri, M. Renfors, "Binary-Offset-Carrier modulation techniques with applications in satellite navigation systems", *Wiley Journal of Wireless Communications and Mobile Computing,* Volume 7, Issue 6, pp. 767-779, Aug. 2007.

[38] J. W. Betz, "The offset carrier modulation for GPS modernization", *Proc. of ION Technical meeting*, pp. 639-648, January 1999, San Diego, CA, USA.

[39] G. W. Hein, J. A. Avila-Rodriguez, S. Wallner, A. R. Pratt, J. Owen, J. Issler, J. W. Betz, C. J. Hegarty, S. Lenahan, J. J. Rushanan, A. L. Kraay, T. A. Stansell, "MBOC: The new optimized spreading modulation recommended for GALILEO L1 OS and GPS L1C", *Proc. of IEEE/ION PLANS,* pp. 883-892, April 2006, San Diego, CA, USA.

[40] M. Fantino, G. Marucco, P. Mulassano, M. Pini, "Performance analysis of MBOC, AltBOC and BOC modulations in terms of multipath effects on the carrier tracking loop within GNSS receivers", *Proc. of IEEE/ION on Position, Location and Navigation Symposium,* pp. 369-376, May 2008, Monterey, CA, USA.

[41] D. Skournetou, E. S. Lohan, "Ionosphere-corrected range estimation in dual-frequency GNSS receivers", *IET Radar, Sonar and Navigation journal,* pp. 215-224, March 2011, Volume 5, Issue 3

[42] E. S. Lohan, "Analytical performance of CBOC-modulated Galileo E1 signal using sine BOC(1,1) receiver for mass-market applications", *published in Position Location and Navigation Symposium (PLANS),2010 IEEE/ION*, pp. 245-253, May 2010, Indian Wells, CA, USA.

[43] J. Zhang, E. S. Lohan, "Effect and mitigation of narrowband interference on Galileo E1 signal acquisition and tracking accuracy", *published in Localization and GNSS (ICL-GNSS), 2011 International Conference,* pp. 36-41, June 2011, Tampere, Finland.

[44] U. Engel, "A theoretical performance analysis of the modernized GPS signals", *Proc. of IEEE/ION Position, Location and Navigation Symposium,* pp. 1067-1078, May 2008, Monterey, CA, USA.

[45] J. A. Rodriguez, G. W. Hein, S. Wallner, J. L. Issler, L. Ries, L. Lestarquit, A. de Latour, J. Godet, F. Bastide, T. Pratt, J. I. R. Owen, "The MBOC Modulation: The Final Touch to the Galileo Frequency and Signal Plan", *NAVIGATION, Journal of The Institute of Navigaiton,* pp. 14-28, Vol. 55, No. 1, Spring 2008.

[46] Status of Galileo and EGNOS, *Presentation at the 7$^{th}$ annual meeting of the International Committee on GNSS (ICG-7)*, November 17-22, 2012, Beijing, China.

[47] *European Space Agency (ESA),* http://www.esa.int/Our_Activities/Navigation/The_future_-_Galileo/Galileo_services, accessed on 30th Jan, 2014.

[48] A. Lewandowski, B. Niehoefer, C. Wietfeld "Galileo/SAR: Performance aspects and new service capabilites", *International Journal of Satellite Communications and Networking, Volume 29, Issue 5,* pp. 441-460, Sept./Oct. 2011.

[49] *Galileo Signal Plan,* www.navipedia.net.

[50] *Federal Space Agency Information – Analytical Centre,* www.glonass-iac.ru/en/.

[51] *European GNSS Service Centre,* www.gsc-europa.eu.

[52] *Global Positioning System, GPS LAB,* was.standford.edu.

[53] D. Zinkiewicz, B. Buszke, M. Houdek, F. Toran-Marti, A. R. Mathur, K. Urbanska, "SISNeT as a source of EGNOS information: Overview of functionalities and applications", *Published in Satellite Navigation Technologies and European Workshop on GNSS Signals and Signal Processing (NAVITEC), 2010 5th ESA Workshop,* pp. 1-7, Dec. 2010, Noordwijk, Netherlands.

[54] M. Z. H. Bhuiyan, S. Söderholm, S. Thombre, L. Ruotsalainen, and H. Kuusniemi, "Implementation of a Software-defined BeiDou Receiver," *Proc. of Chinese Satellite Navigation Conference' 2014, Volume 202,* pp. 751-762, 21-23 May, 2014, Nanjing, China.

[55] M. Z. H. Bhuiyan and E. S. Lohan, "Multipath Mitigation Techniques for Satellite-Based Positioning Applications", *book chapter17 in S. Jin (Ed),* "Global Navigation Satellite Systems: Signal, Theory and Applications", ISBN978-953-307-843-4, InTech, February 2012.

[56] M. Z. H. Bhuiyan and E. S. Lohan, "Advanced multipath mitigation techniques for satellite-based positioning applications", *in Hindawi International Journal on Navigation and Observation, Volume 2010 (2010),* ArticleID 412393, 15 pages, doi:10.1155/2010/412393, http://www.hindawi.com/journals/ijno/2010/412393 .html.

[57] E. S. Lohan, A. Lakhzouri, and M. Reinfors, "Feedforward delay estimators in adverse multipath propagation for Galileo and modernized GPS signals", *EURASIP Journal of Applied Signal Processing,* vol. 3006, ArticleID 50971, 19 pages.

[58] M. Pini, G. Falco, L. L. Presti, "Estimation of Satellite-User Ranges Through GNSS Code Phase Measurements", *book chapter 5 in S. Jin (Ed),* "Global Navigation Satellite Systems: Signal, Theory and Applications", ISBN978-953-307-843-4, InTech, February 2012.

[59] H. Kuusniemi, E. Airos, M. Z. H. Bhuiyan, and T. Kröger, "GNSS Jammers: How vulnerable are Consumer Grade Satellite Navigation Receivers?," *European Journal of Navigation*, 08/2012; pp. 14-21; Volume 10 Number 2.

[60] M. Z. H. Bhuiyan, "Analysis of Multipath Mitigation Techniques for Satellite-based Positioning Applications," Ph.D. Thesis, Publication number 981, Tampere University of Technology, Tampere, Finland.